Comparative analysis of ChAdOx1 nCoV-19 and Ad26.COV2.S SARS-CoV-2 vector vaccines

Stephan Michalik,[1*] Florian Siegerist,[2*] Raghavendra Palankar,[3*] Kati Franzke,[4*] Maximilian Schindler,[2] Alexander Reder,[1] Ulrike Seifert,[5] Clemens Cammann,[5] Jan Wesche,[3] Leif Steil,[1] Christian Hentschker,[1] Manuela Gesell-Salazar,[1] Emil Reisinger,[6] Martin Beer,[7#] Nicole Endlich,[2#] Andreas Greinacher[3#] and Uwe Völker[1#]

[1]Interfaculty Institute of Genetics and Functional Genomics, Department of Functional Ge-nomics, University Medicine Greifswald, Greifswald; [2]Institute for Anatomy and Cell Biology, University Medicine Greifswald, Greifswald; [3]Institute of Transfusion Medicine, University Medicine Greifswald, Greifswald; [4]Institute of Infectiology, Friedrich-Loeffler-Institut, Greifswald-Insel Riems; [5]Friedrich Loeffler-Institute of Medical Microbiology-Virology, University Medicine Greifswald, Greifswald; [6]Division of Tropical Medicine and Infectious Diseases, Center of Internal Medicine II, Rostock University Medical Center, Rostock, and [7]Institute of Diagnostic Virology, Friedrich-Loeffler-Institut, Greifswald-Insel Riems, Germany

**SM, FS, RP and KF contributed equally as co-first authors*

#MB, NE, AG and UV contributed equally as co-senior authors

 doi:10.3324/haematol.2021.280154

Received: October 5, 2021.

Accepted: January 5, 2022.

Pre-published: January 20, 2022.

Correspondence: *ANDREAS GREINACHER* - andreas.greinacher@med.uni-greifswald.de

UWE VÖLKER - voelker@uni-greifswald.de

Comparative analysis of ChAdOx1 nCoV-19 and Ad26.COV2.S SARS-CoV-2 vector vaccines

Supplemental Material

Stephan Michalik[1,*], Florian Siegerist[2,*], Raghavendra Palankar[3,*], Kati Franzke[4,*], Maximilian Schindler[2], Alexander Reder[1], Ulrike Seifert[5], Clemens Cammann[5], Jan Wesche[3], Leif Steil[1], Christian Hentschker[1], Manuela Gesell-Salazar[1], Emil Reisinger[6], Martin Beer[7,§], Nicole Endlich[2,§], Andreas Greinacher[3,§], Uwe Völker[1,§]

[*]shared first authors

[§]shared last authors

[1]Interfaculty Institute of Genetics and Functional Genomics, Department Functional Genomics, University Medicine Greifswald, Greifswald, Germany

[2]Institute for Anatomy and Cell Biology, University Medicine Greifswald, Greifswald, Germany

[3]Institute of Transfusion Medicine, University Medicine Greifswald, Greifswald, Germany

[4]Institute of Infectiology, Friedrich-Loeffler Institut, Greifswald-Insel Riems, Germany

[5]Friedrich Loeffler-Institute of Medical Microbiology-Virology, University Medicine Greifswald, Greifswald, Germany.

[6]Division of Tropical Medicine and Infectious Diseases, Center of Internal Medicine II, Rostock University Medical Center, Rostock, Germany

[7]Institute of Diagnostic Virology, Friedrich-Loeffler Institut, Greifswald-Insel Riems, Germany

Table of contents

Supplemental Figures

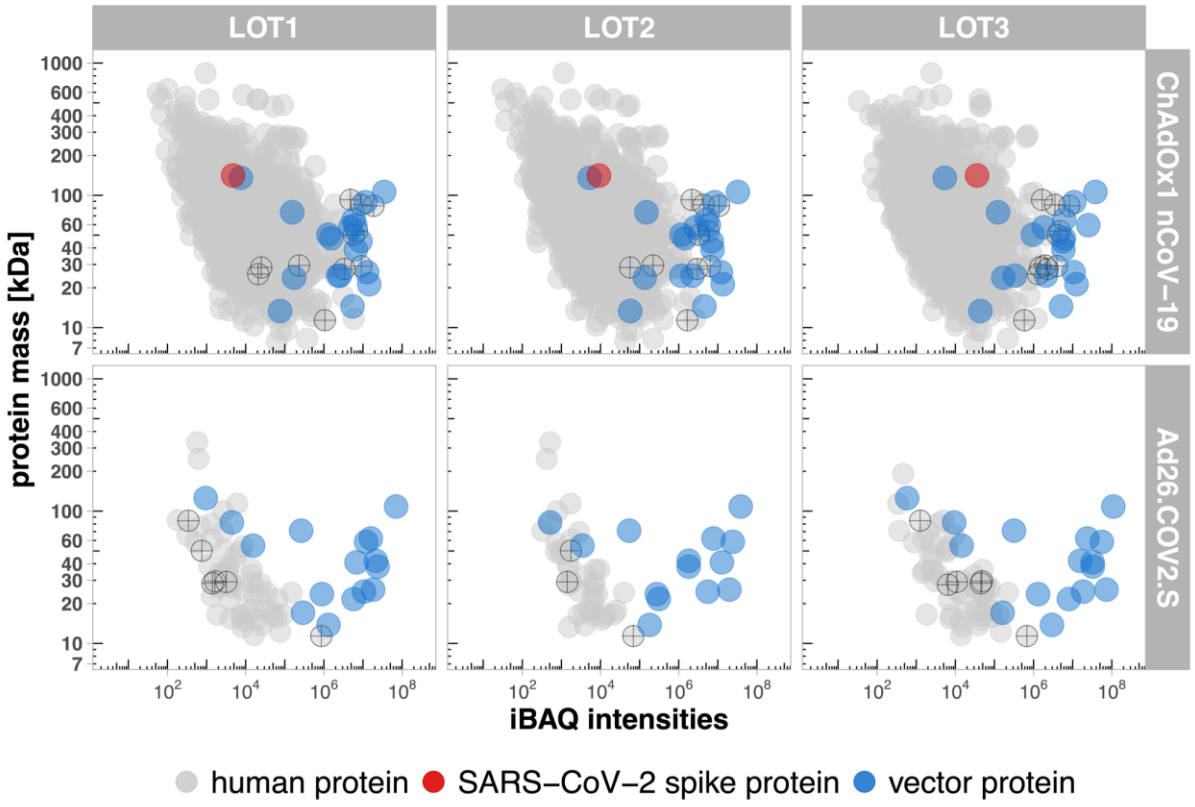

Supplementary Figure 1: Proteome profiling of ChAdOx1 nCoV-19 and Ad26.COV2.S vaccines revealed major differences in host cell protein content

iBAQ protein intensities and theoretical molecular mass of identified proteins. Protein intensities of vaccine lots 1-3 for ChAdOx1 nCoV-19 or Ad26.COV2.S vaccine were calculated using the iBAQ algorithm (min. 3 unique peptides per protein) and plotted against the theoretical molecular mass. Proteins were color-coded according to their respective class. Blue dots indicate vector proteins, gray proteins represent human proteins and the red dot indicates the SARS-CoV-2 spike protein. Points marked with a cross are those used in the Western blot analysis.

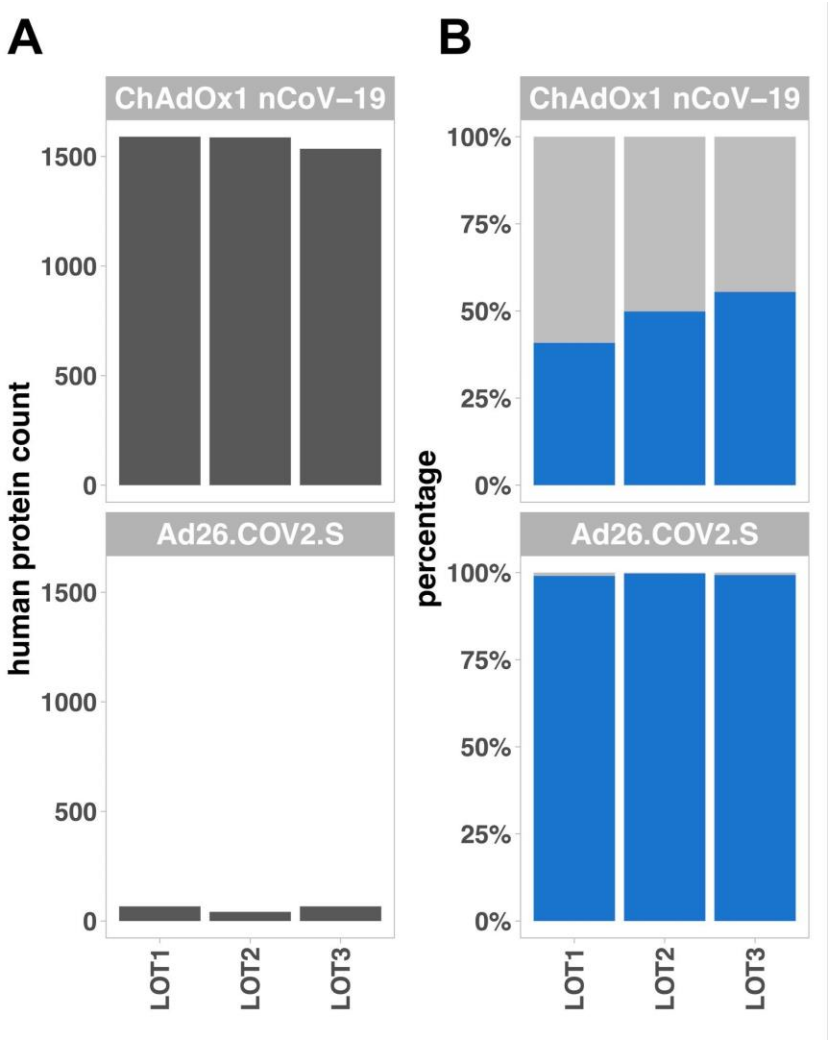

Supplementary Figure 2: Host cell protein count and HCP percentage

(A) Host cell protein (HCP) identification count for ChAdOx1 nCoV-19 or Ad26.COV2.S vaccines. Host cell proteins (HCP) with at least 3 peptides were counted per lot and displayed in a bar plot. **(B)** iBAQ protein intensities of human and vector proteins. For vaccine lots 1-3 for ChAdOx1 nCoV-19 or Ad26.COV2.S, iBAQ protein intensities were summed per protein class and resulting percentages were calculated and displayed in a stacked bar plot (grey = human proteins, blue = vector proteins).

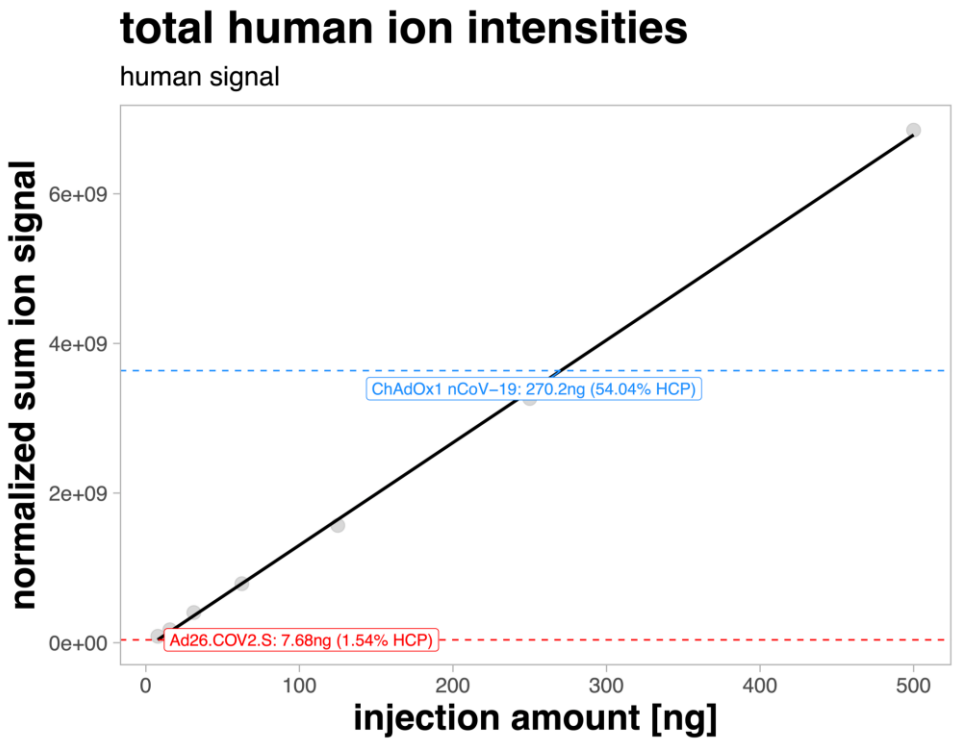

Supplementary Figure 3: HCP DIA-MS analysis of the dilution series of ChAdOx1 nCoV-19 and Ad26.COV2.S vaccines

Normalized sum of identified HEK293 human ion signals per injection amount was used for the linear regression (black line = regression; single points = grey). The ion signals were used to estimate the amount of human signal in 500 ng of vaccine (dashed lines; ChAdOx1 nCoV-19 = blue, Ad26.COV2.S = red).

HSP90 - alpha

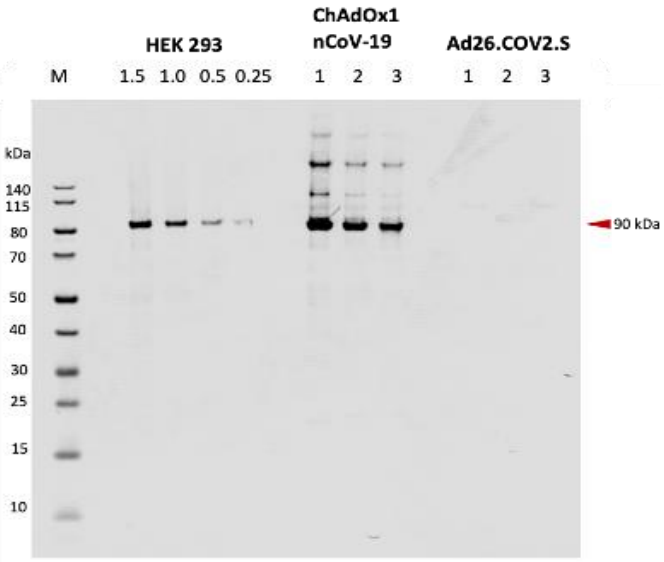

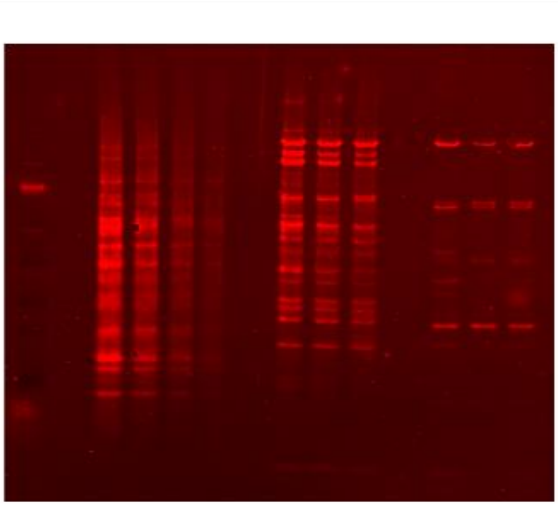

HSP90 - AB1

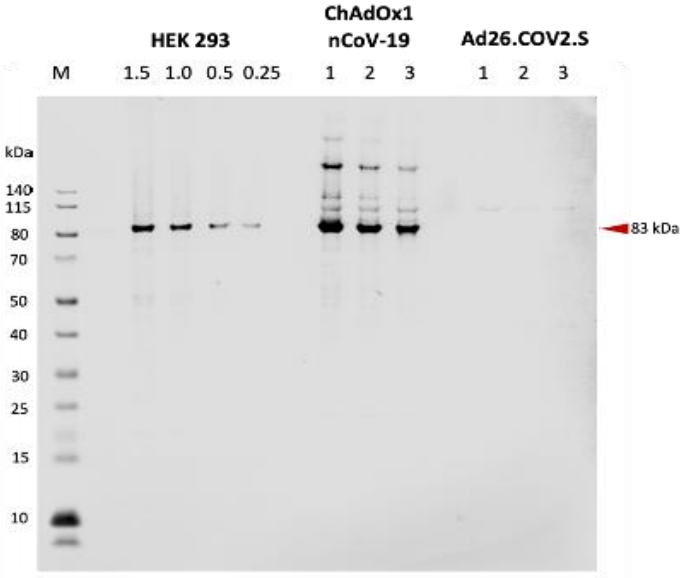

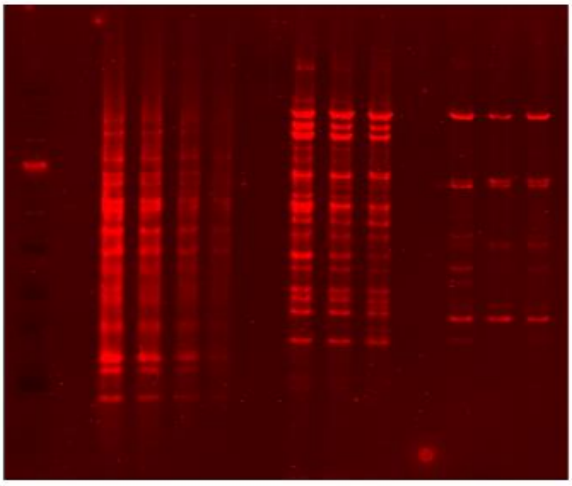

GRP94

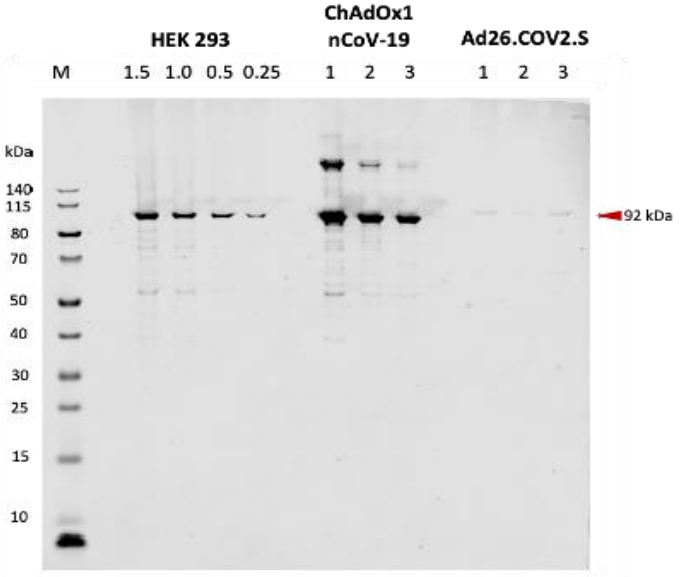

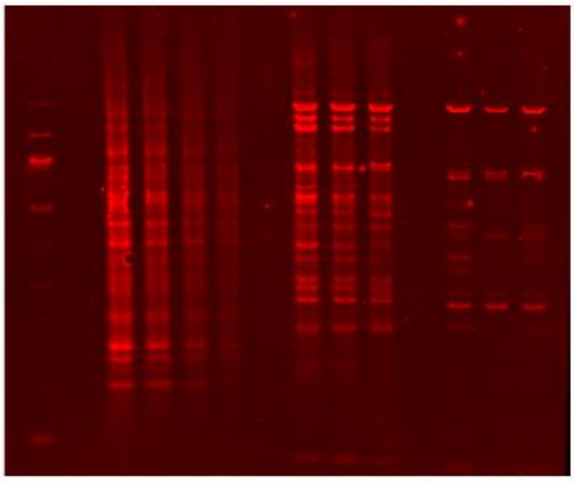

14-3-3 Epsilon

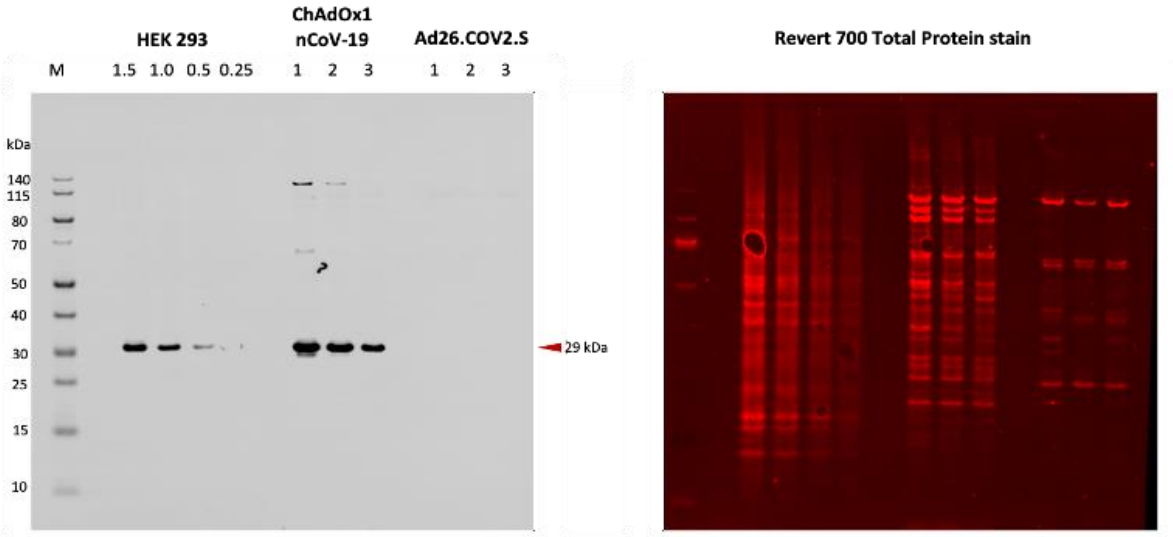

Tubulin alpha-1B

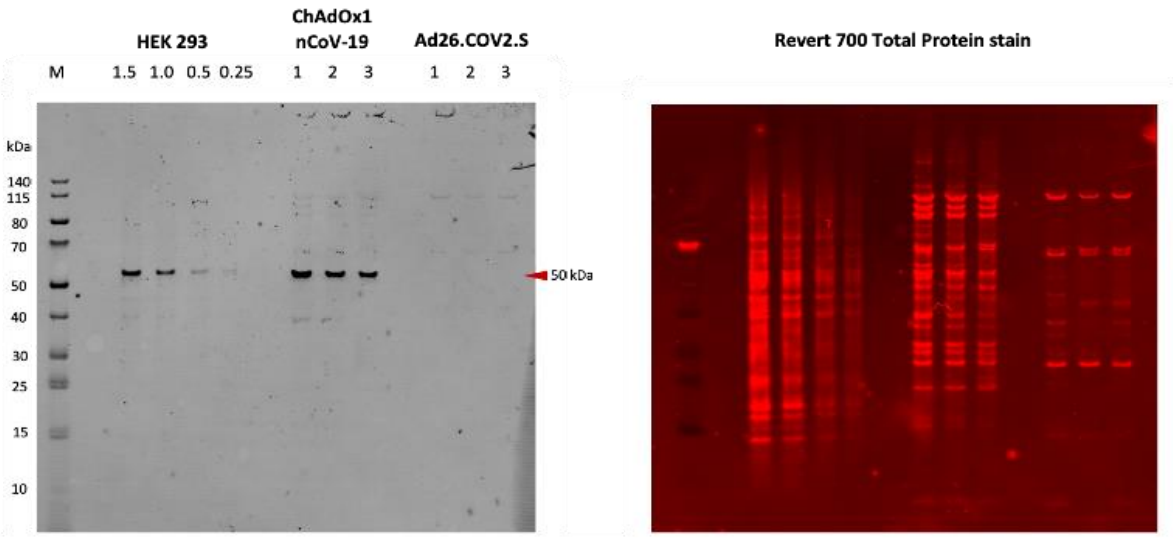

YWHAZ

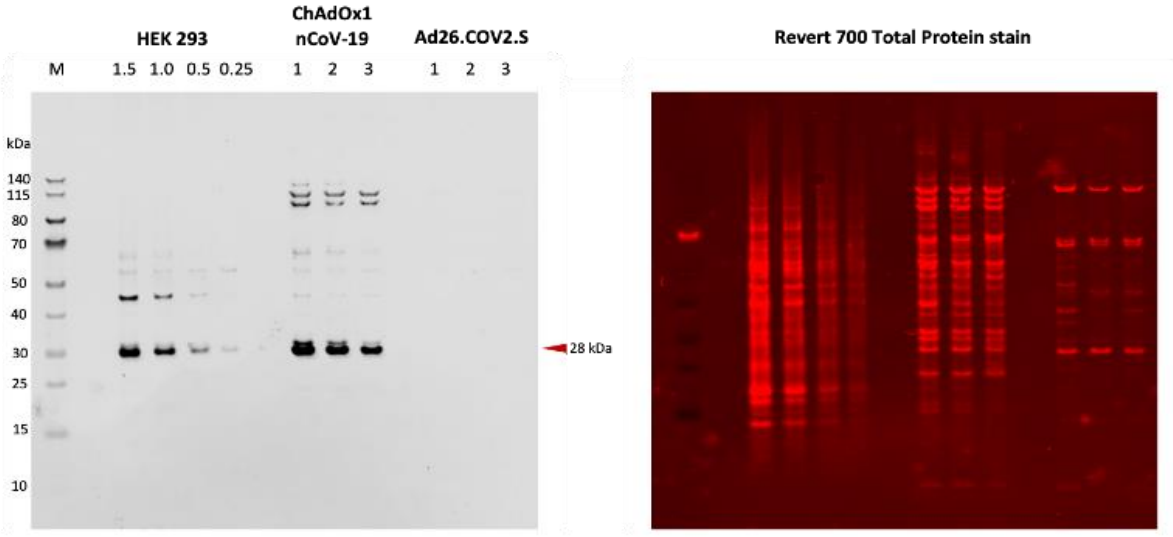

Vimentin

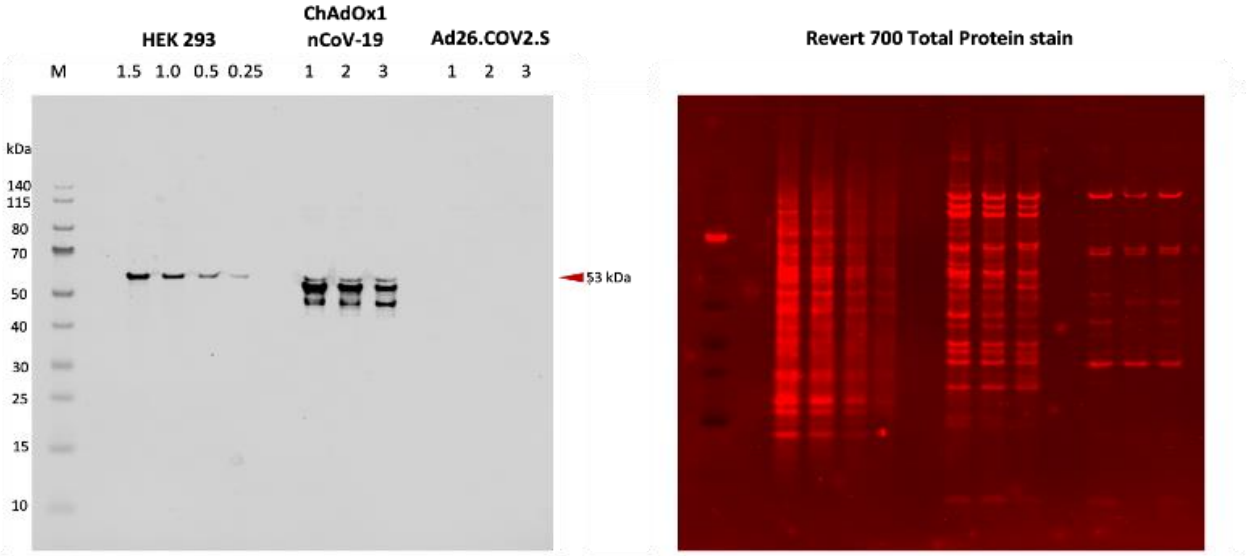

Histone H4

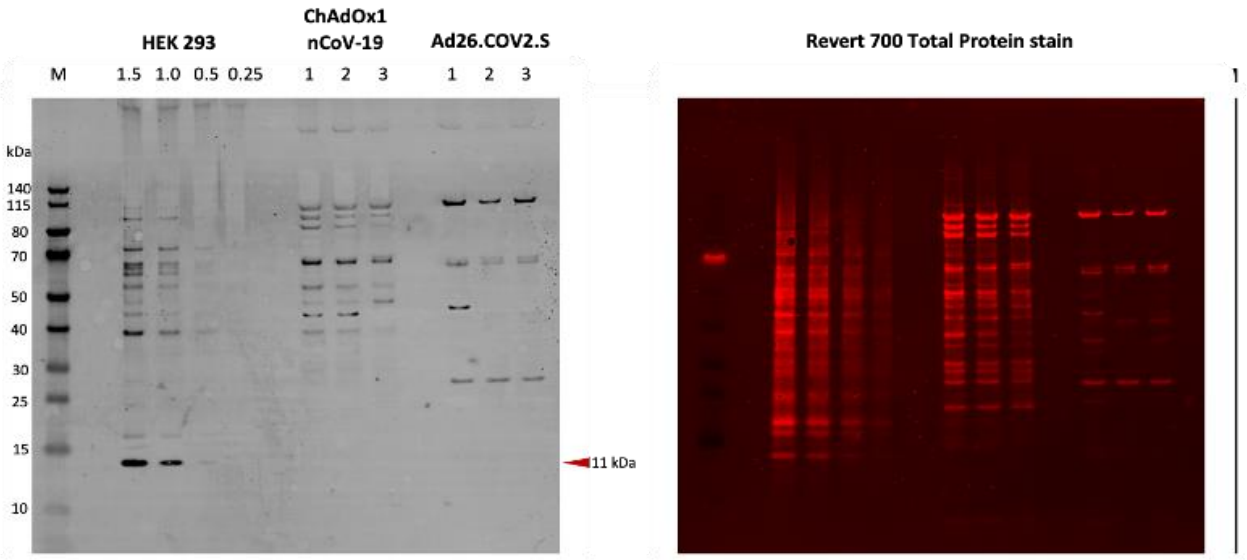

PSMB5 – MB1

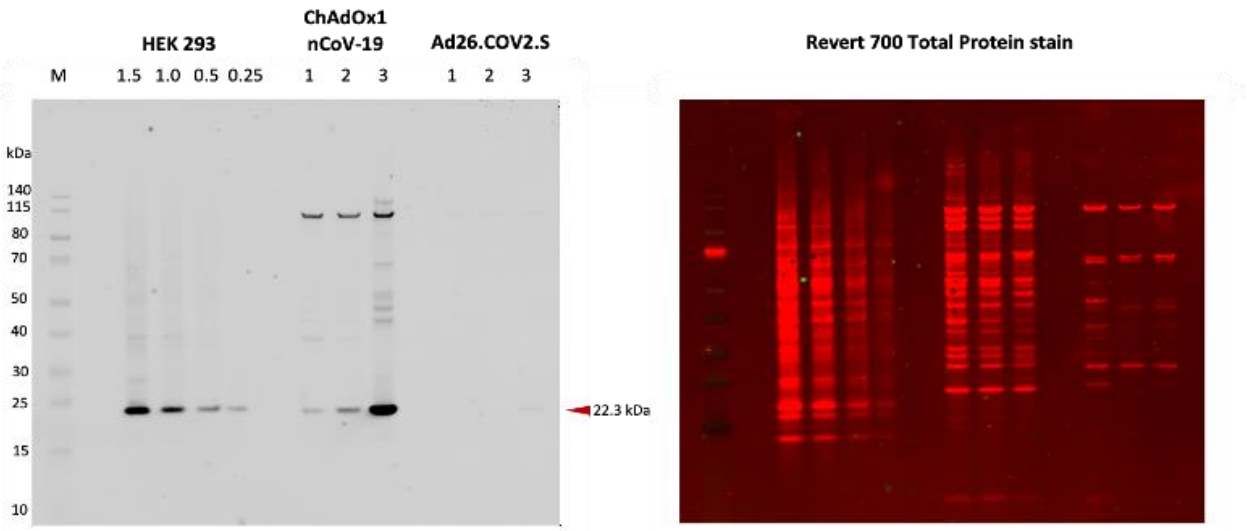

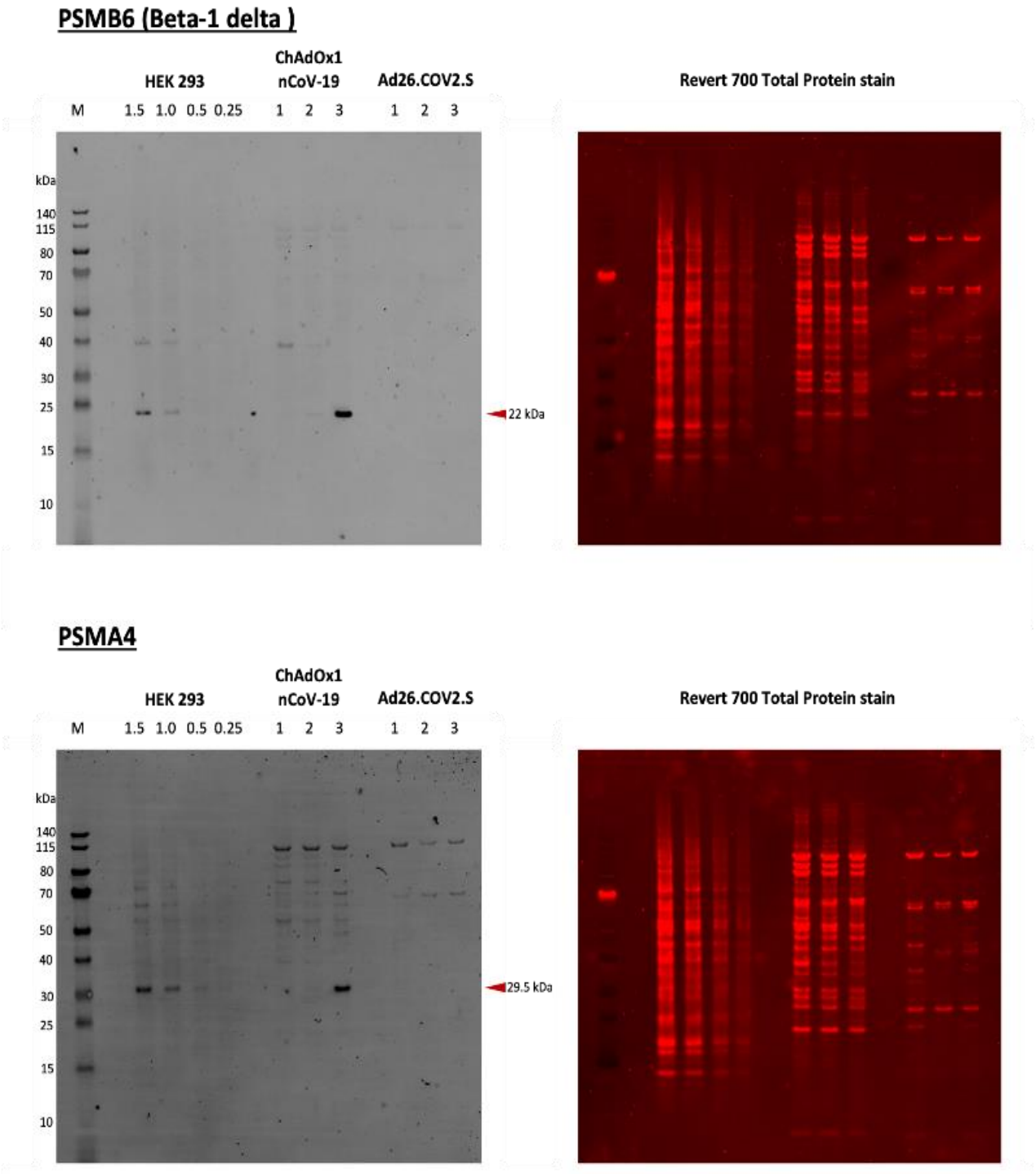

Supplementary Figure 4: Western blot analysis

Western blot results (left panels) and corresponding Revert 700 total protein stains as a transfer control (right panels) of a dilution series of a laboratory HEK293 cell line extract [1.5, 1.0, 0.5 and 0.25 µg] for direct comparison to 10 µL (1/50th of a vaccine dose) of 3 lots of ChAdOx1 nCoV-19 and Ad26.COV2.S vaccines, respectively. Antibody specificity is indicated on the top left and the respective specific signal is indicated by a red arrowhead and the expected molecular weight (in kDa) of the target protein. Western blots of the target proteins are shown in the order HSP90-alpha, HSP90-AB1, GRP94, 14-3-3 epsilon, tubulin alpha-1B, YWHAZ, vimentin, histones H4, PSMB5-MB1, PSMB6 (beta-1 delta) as well as PSMA4.

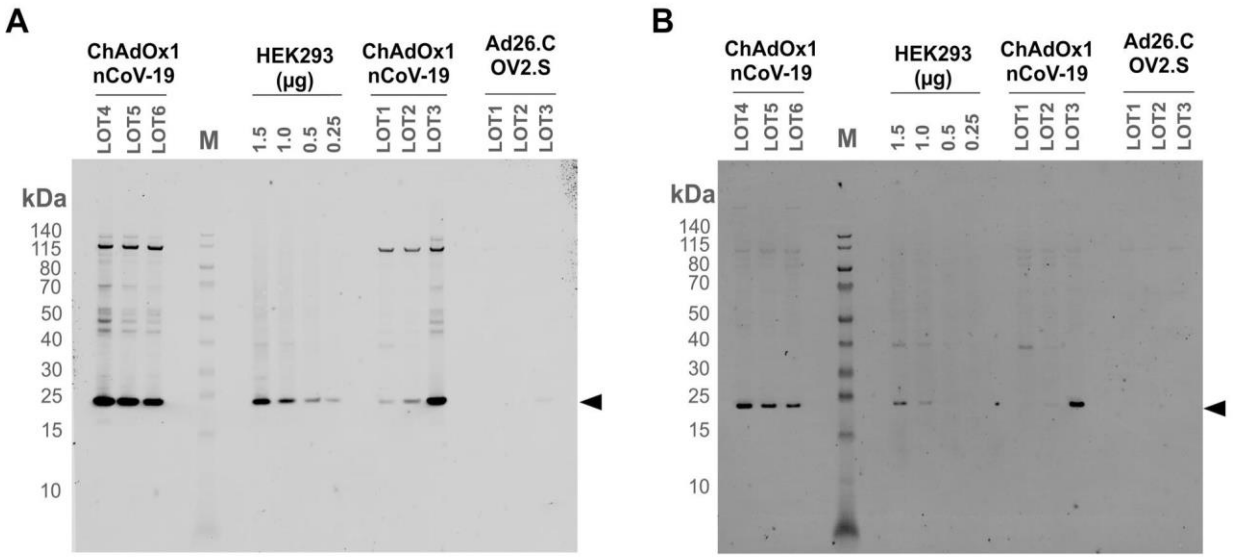

Supplementary Figure 5: Western blot analysis of protein proteasome subunit abundances in vaccines

(A) Western blot shown for proteasome subunit beta type-5 protein (PSMB5 - MB1). **(B)** Western blot shown for proteasome subunit beta type-6 protein (PSMB6 - Beta-1 delta). ChAdOx1 nCoV-19 lot 6 was not included in the calculations because no proteasome activity measurement is available for this lot.

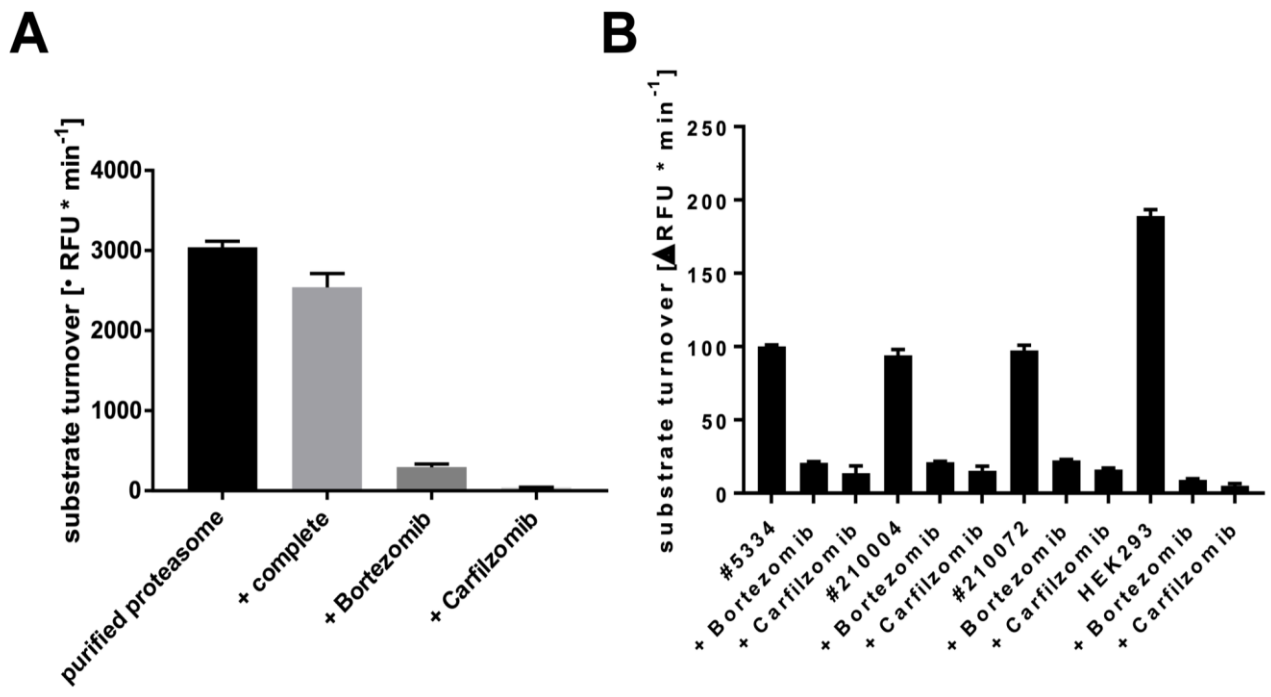

Supplementary Figure 6: proteasome inhibitor control experiments

(A) Chymotrypsin-like activity of standard proteasomes isolated from human erythrocytes was measured in assay buffer containing 30mM Tris pH 7.5, 5mM $MgCl_2$, 10mM KCl, 10% Glycerol and protease inhibitor cocktail Complete (Sigma-Aldrich) or in the presence of either 100 nmol/L bortezomib or 200 nmol/L carfilzomib (n = 3, technical replicates) **(B)** Chymotrypsin-like activity of three lots ChAdOx1 nCoV-19 (#5334, 210072 and #210004, $1/10^{th}$ of vaccination dose) was compared with the activity of 0.25 µg HEK293 cell lysate. As control for specific proteasome inhibition carfilzomib was added and displayed slightly more inhibition compared to bortezomib (n=3, technical replicate).

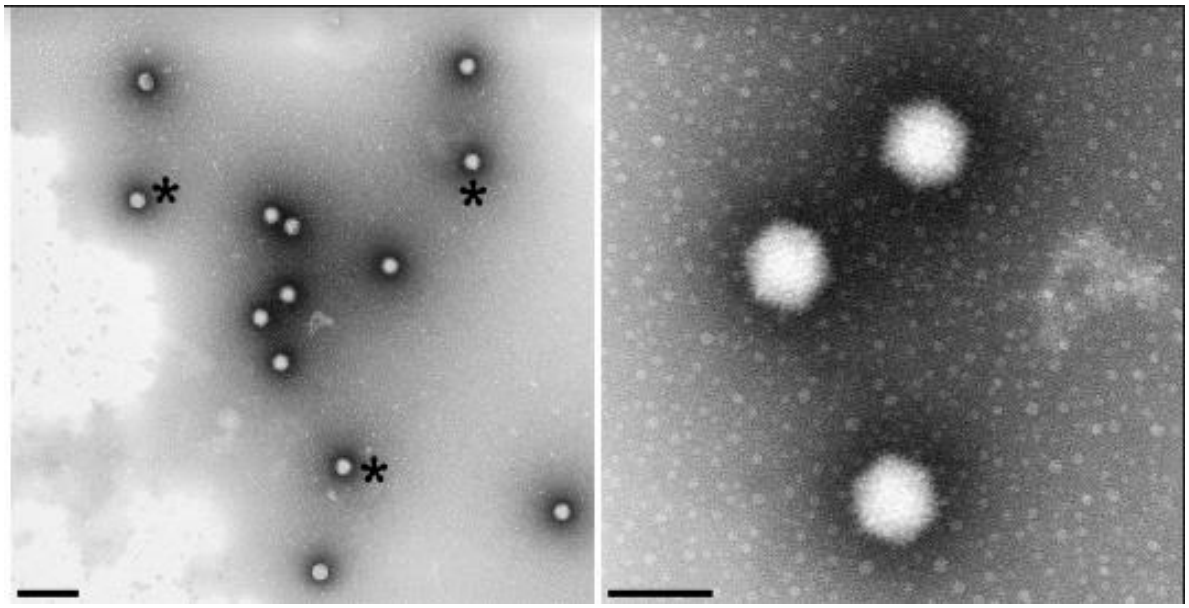

Supplementary Figure 7: Electron micrograph of purified adenovirus particles from ChAdOx1 nCov-19 vaccine in different magnifications

Asterisks exemplarily indicate adenoviral particles. Scale bars represent 300 nm and 100 nm from left to right panel.

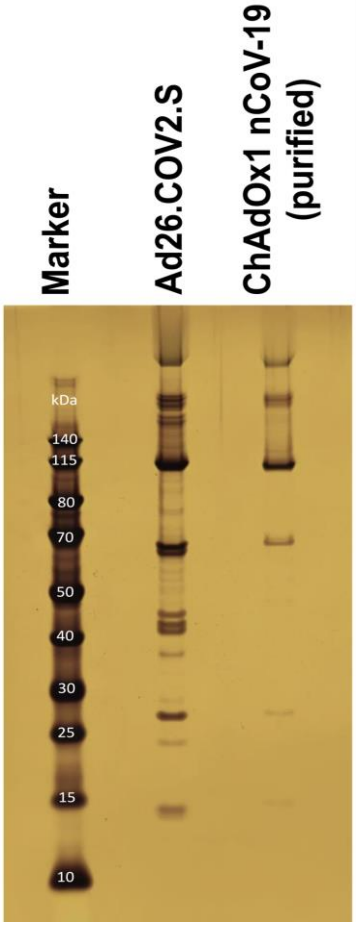

Supplementary Figure 8: Protein pattern of the Ad26.COV2.S and the purifiedChAdOx1 nCoV-19 vaccine

A silver nitrate-stained SDS-PAGE gel is shown for Ad26.COV2.S and purified ChAdOx1 nCoV-19. First lane: molecular weight marker, second lane: 10 µL Ad26.COV2.S. third lane: 4 µl aliquot of ChAdOx1 nCov-19 purification from density gradient centrifugation.

A. Hydrodynamic diameter of ChAdOx1 nCoV-19 incubated with increasing concentrations of PF4.

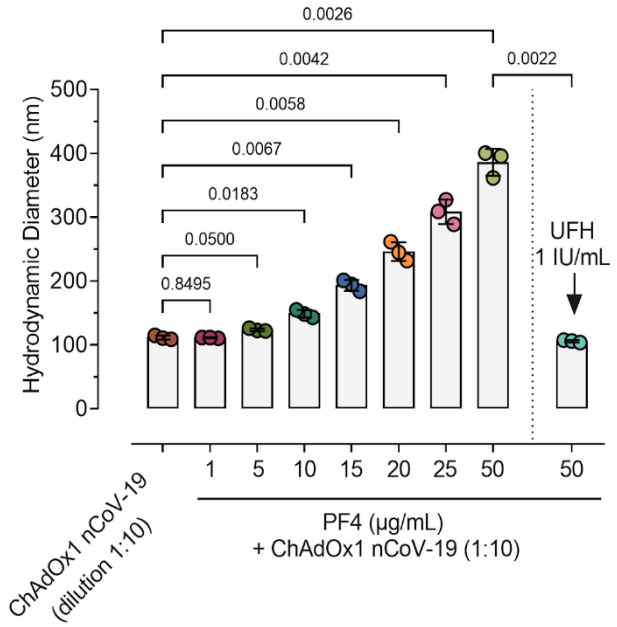

B. Hydrodynamic diameter of Ad26.COV2.S incubated with increasing concentrations of PF4.

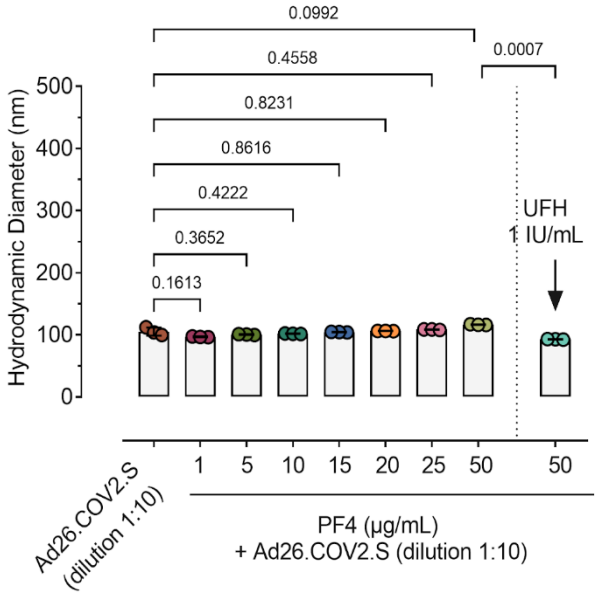

Supplementary Figure 9: Comparison of hydrodynamic diameter of ChAdOx1 nCov-19 vaccine and Ad26.COV2.S vaccine incubated with increasing concentrations of PF4

(A) ChAdOx1 nCov-19 vaccine and its supernatant incubated with PF4 shows a concentration dependent exponential increase in hydrodynamic diameter measured by DLS but not with (B) Ad26.COV2.S vaccine. Complexes formed between PF4 and vaccine or its components are disrupted by UHF (1 IU/mL).

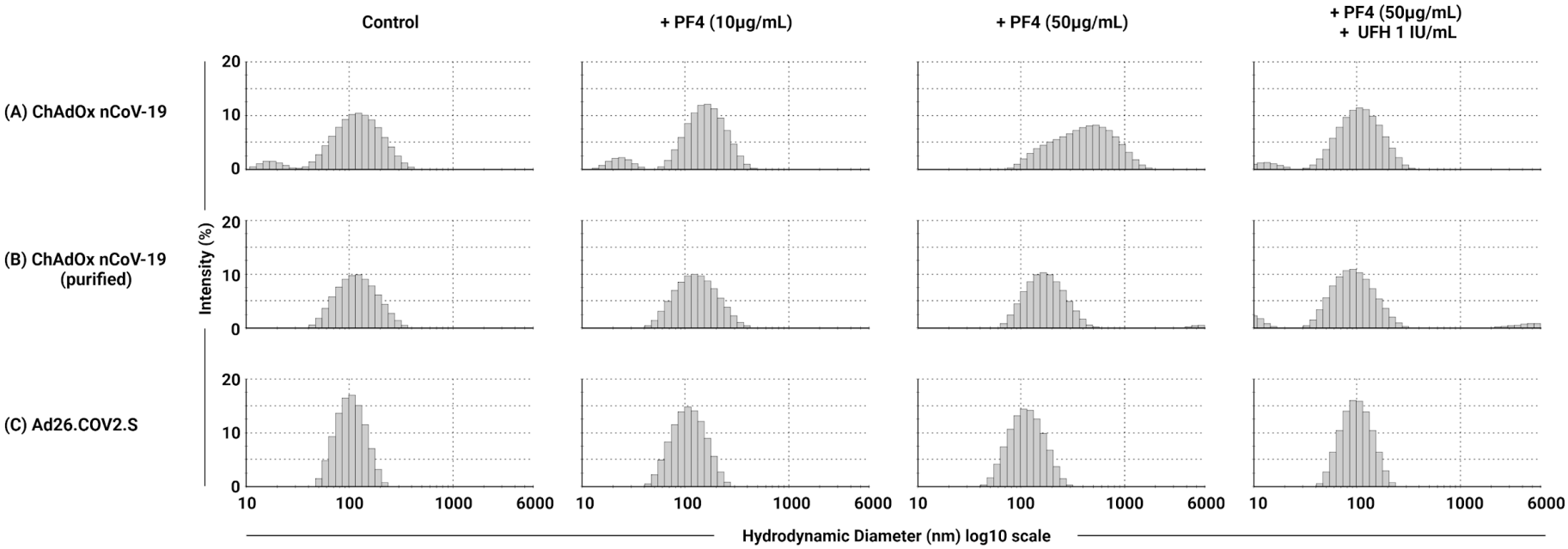

Supplementary Figure 10: Representative percent intensity histogram of the hydrodynamic diameter from DLS

Changes in hydrodynamic diameter of (A) ChAdOx1 nCoV-19, (B) purified ChAdOx1 nCoV-19 and (C) Ad26.COV2.S vaccine incubated and in complex with PF4 (10 µg/mL and 50 µg/mL) and dissociation of the complexes after the addition of UFH (1 IU/mL)

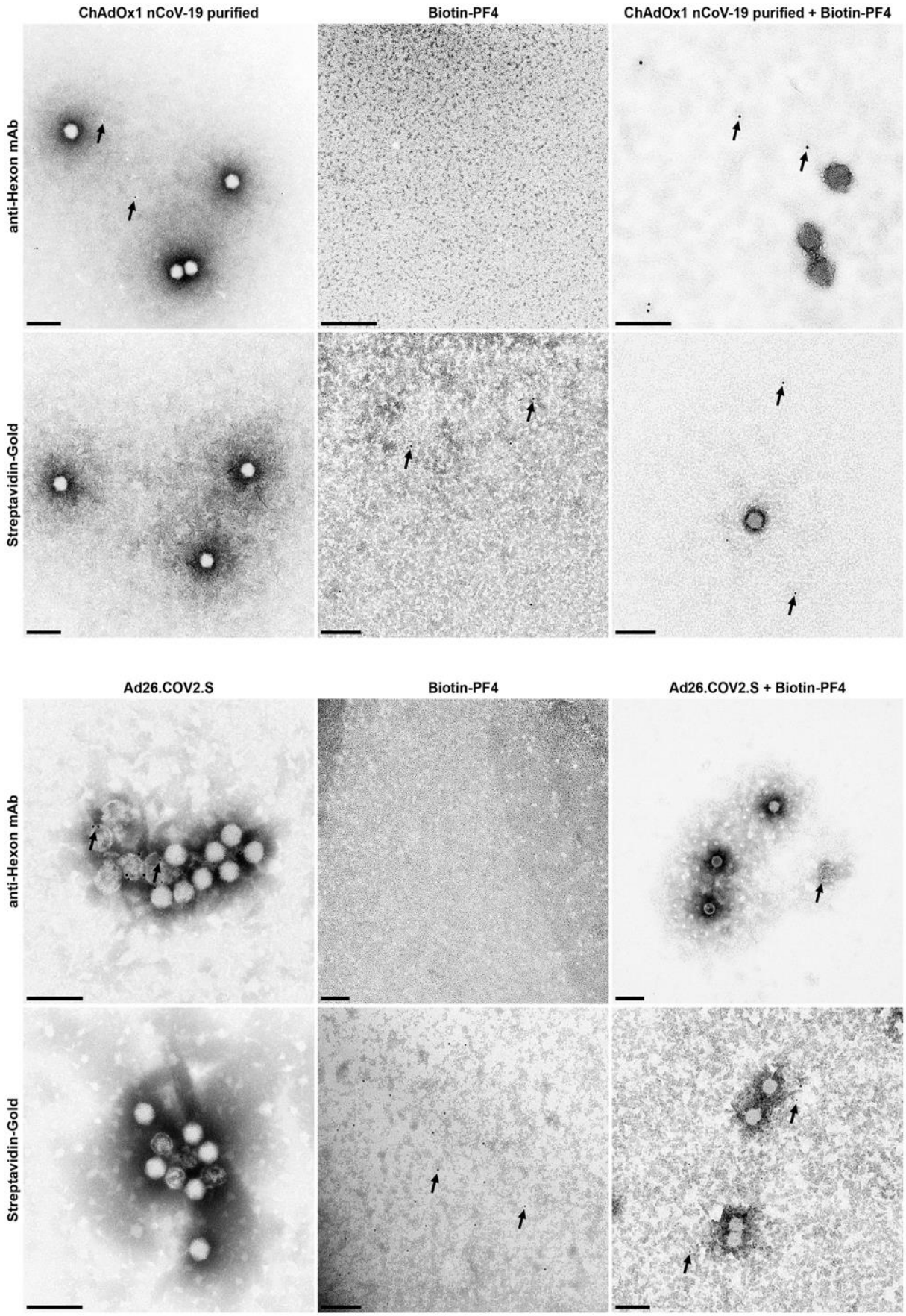
ChAdOx1 nCoV-19 purified
Biotin-PF4
ChAdOx1 nCoV-19 purified + Biotin-PF4
anti-Hexon mAb
Streptavidin-Gold
Ad26.COV2.S
Biotin-PF4
Ad26.COV2.S + Biotin-PF4
anti-Hexon mAb
Streptavidin-Gold

Supplementary Figure 11: Purified ChAdOx1 nCov-19 vaccine and Ad26.COV2.S incubated with biotinylated PF4 and stained with anti-hexon mAb and streptavidin-gold conjugate

In immunoelectron microscopy the anti-hexon mAb binds to an epitope that is located inside the capsid of an intact virion. Binding events were only seen with defect virions or not assembled hexon protein. Arrows indicate single gold particles. Bars represent 200 nm.

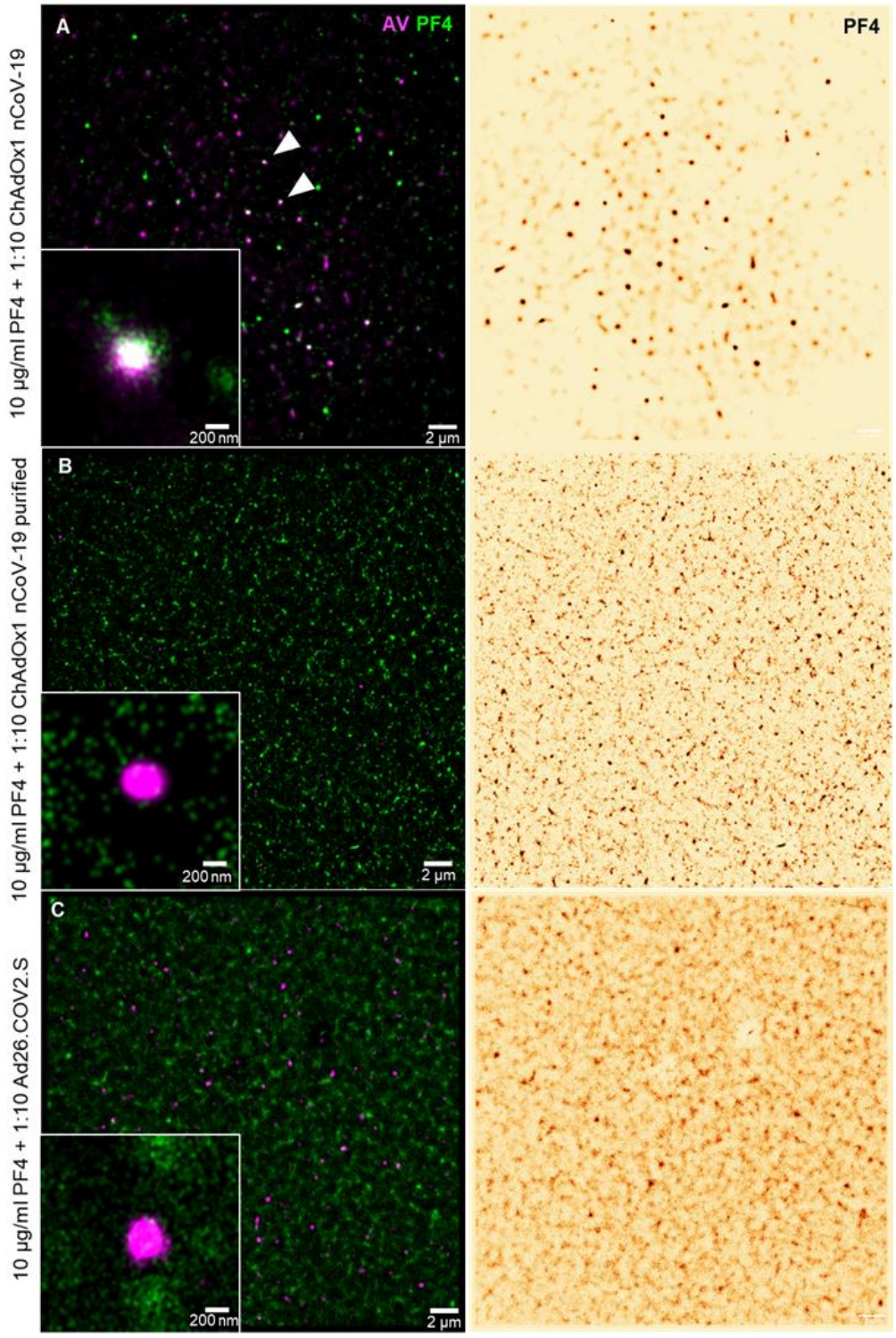

Supplementary Figure 12: Dual-channel SMLM for hexon and PF4: Average shifted histograms

Full field of view of immuno-labeled PF4 and hexon polypeptide after incubation with either native ChAdOx1 nCoV-19 **(a)**, purified ChAdOx1 nCoV-19 **(B)** or Ad26.COV2.S **(C)** acquired by SMLM and reconstructed as average shifted histograms. After incubation with ChAdOx nCoV-19 (A), PF4 can be visualized as dense clusters that colocalize with the hexon polypeptide (arrowheads). In contrast, after incubation with either purified ChAdOx1 nCoV-19 (B) or Ad26.COV2.S (C), PF4 formed a rather homogenous layer on glass slides and only single and small complexes were found.

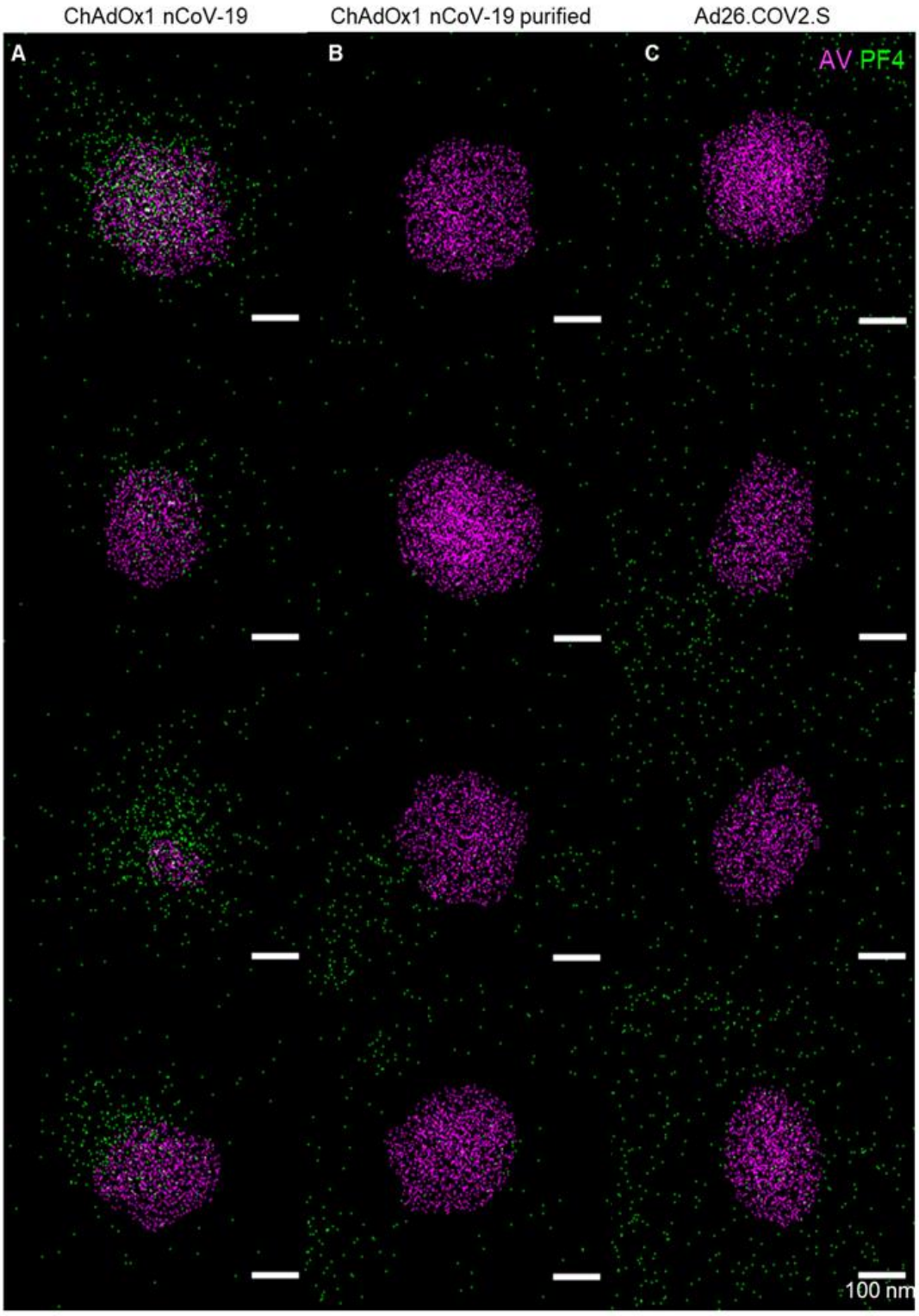

Supplementary Figure 13: Dual-channel single-molecule scatterplots of the PF4 (green) and the adenoviral hexon polypeptide (magenta)

Herein, each spot represents one fluorophore localization. Clearly, distinct clustering of PF4 molecules can only be seen in native ChAdOx1 nCoV-19 **(A)** which shows a high PF4 density either directly on, or in direct vicinity of particles staining for hexon proteins. In contrast PF4 molecule density is very similar inside or outside hexon-localizations in purified ChAdOx1 nCoV-19 and Ad26.COV2.S **(B, C)**. For comparative quantification of molecule density see main Figure 4, G.

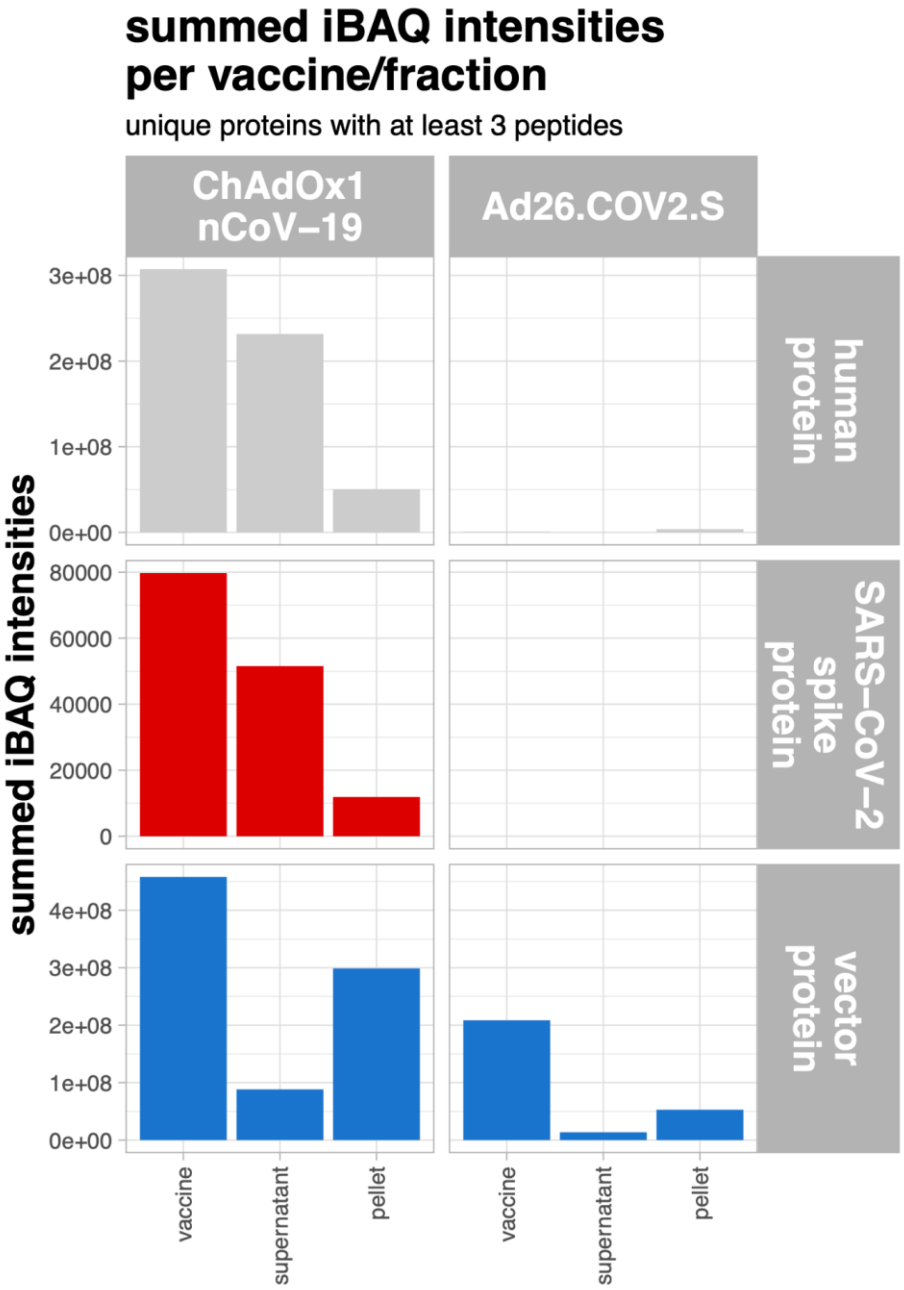

Supplementary Figure 14: Comparison of summed iBAQ protein intensities per sub-proteome before and after purification of virions of ChAdOx1 nCoV-19 and Ad26.COV2.S

iBAQ protein intensities were summed per protein class and resulted intensity values were displayed in a barplot (grey = human proteins, blue = vector proteins, red = SARS-CoV-2 spike protein).

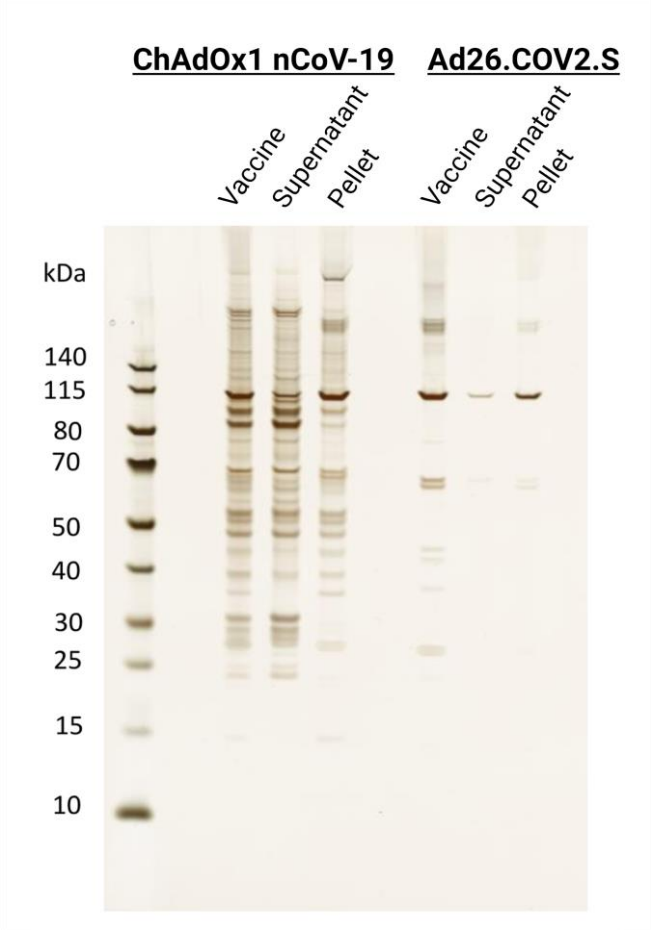

Supplementary Figure 15. Silver nitrate stained SDS-PAGE of fractionated vaccines

Protein patterns of silver nitrate-stained SDS-PAGE of 1/50th of a vaccine dose of the untreated vaccine as well as the supernatant and the pellet fraction after ultracentrifugation of the ChAdOx1 nCoV-19 (left) and Ad26.COV2.S (right) vaccines.

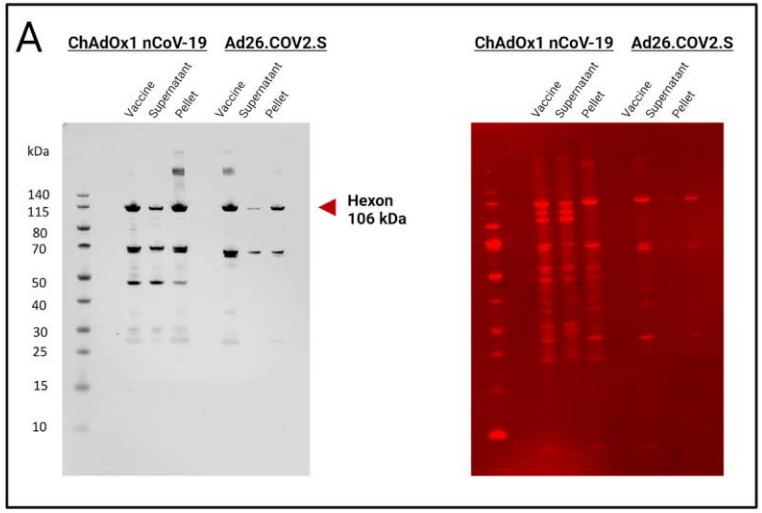
A
ChAdOx1 nCoV-19
Ad26.COV2.S
Vaccine
Supernatant
Pellet
kDa
140
115
80
70
50
40
30
25
15
10
Hexon
106 kDa

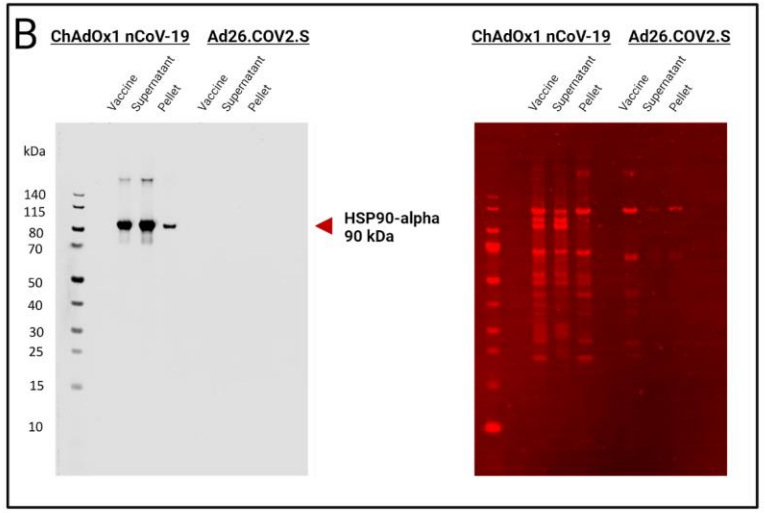
B
ChAdOx1 nCoV-19
Ad26.COV2.S
Vaccine
Supernatant
Pellet
kDa
140
115
80
70
50
40
30
25
15
10
HSP90-alpha
90 kDa

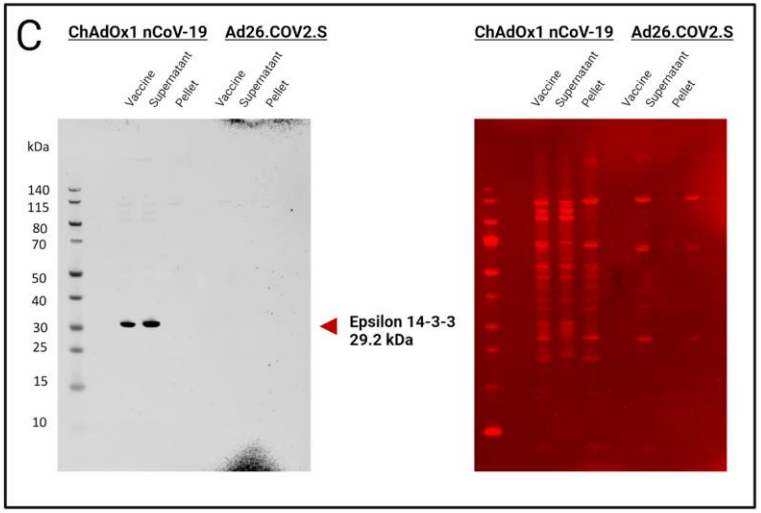
C
ChAdOx1 nCoV-19
Ad26.COV2.S
Vaccine
Supernatant
Pellet
kDa
140
115
80
70
50
40
30
25
15
10
Epsilon 14-3-3
29.2 kDa

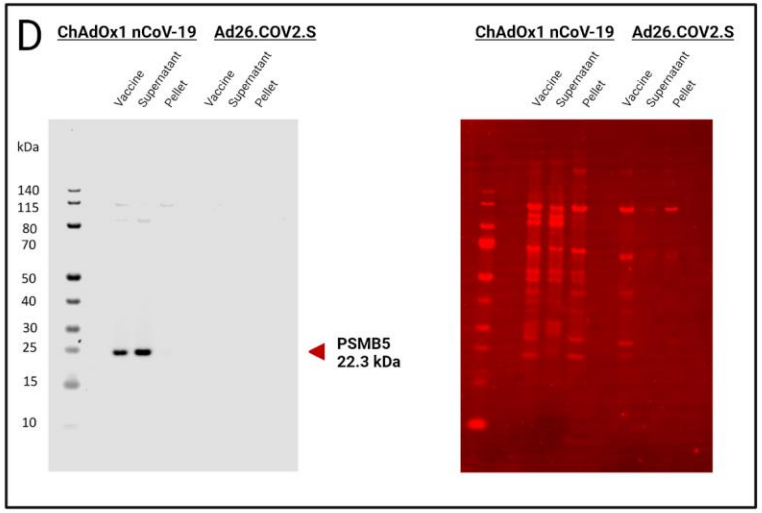
D
ChAdOx1 nCoV-19
Ad26.COV2.S
Vaccine
Supernatant
Pellet
kDa
140
115
80
70
50
40
30
25
15
10
PSMB5
22.3 kDa

Supplementary Figure 16. Western blot analysis of the fractionated vaccines

Western blot results with their corresponding Revert 700 total protein stains as a transfer control of 1/50th of a vaccine dose of the untreated vaccine as well as the supernatant and the pellet fraction after ultracentrifugation of the ChAdOx1 nCoV-19 and Ad26.COV2.S vaccines. Antibody specificity A) Anti-Hexon, B) anti-HSP90-alpha, C) anti-Epsilon 14-3-3, D) anti PSMB5 and the specific target protein signals are indicated by red arrowheads and the expected molecular weight (in kDa).

Supplemental Table 1

Supplemental table 1 contains the resulting iBAQ intensities of identified proteins of the comparison of ChAdOx1 nCoV-19 and Ad26.COV2.S.

Supplemental Table 2

Top10 human protein impurities for ChAdOx1 and Ad26.COV2.S vaccine based on mean iBAQ protein intensity per vaccine. The red-white-green iBAQ color gradient shows the iBAQ intensities from high-middle-low abundant proteins respectively.

Supplementary Video 1

Supplementary video 1 shows intramuscular microinjections in adjacent myotomes of a zebrafish tail. Special care was taken not to injure the adjacent caudal vein or segmental arteries.

Supplementary Materials and Methods

Sample preparation for LC-MS/MS analysis

Vaccines were precipitated using a quantitative salt-acetone precipitation[1] and the precipitate was resuspended in one-fifth of the initial volume using 20 mM HEPES buffer pH 8 containing 1 % (w/v) SDS.

Determination of protein concentrations was performed using a microBCA assay according to the manufacturer's instructions (Pierce Thermo Fisher, Bonn, Germany).

2 µg of protein was reduced (2.5 mM DTT ultrapure, Invitrogen/Thermo Fisher, Bonn, Germany) for 30 minutes at 37 °C and alkylated (10 mM iodoacetamide for 15 minutes at 37 °C, Sigma Aldrich, Munich, Germany). Subsequently, protein was digested with trypsin (enzyme to protein ratio of 1:25) on SP3 beads as described by Blankenburg *et al.*[2]

SDS gel and Western blot analysis

For protein separation, 2 µl of the three precipitated ChAdOx1 nCoV-19 (lot 1 – 1.14 µg, lot 2 – 1.05 µg, lot 3 – 0.86 µg) and Ad26.COV2.S vaccine samples (lot 1 – 0.39 µg, lot 2 – 0.3 µg, lot 3 – 0.2 µg) corresponding to one fiftieth of one vaccine dose as well as dilutions of HEK293 total protein lysate (1.5, 1.0, 0.5 and 0.25 µg) were adjusted to 10 µl sample volume with water and 4x SDS-PAGE sample buffer (Licor D00317-01) with added mercaptoethanol [10 %]. Accordingly, 0.5 µl of size standard (PageRuler Prestained Protein Ladder, Invitrogen/Thermo Fisher) was adjusted to a final volume of 10 µl with water and 4x SDS-sample buffer. Samples and standard were denatured for 2 min at 95 °C, chilled to room temperature and loaded to a precast NuPAGE™ 4 to 12 %, Bis-Tris Midi Gel 1.0 mm x 26 well (WG1403BX10, Invitrogen/Thermo Fisher). Electrophoresis was performed at 150 V using a Power Pack 200 (BioRad, Hercules, CA, USA) and a Criterion Cell (BioRad). All reagents and buffers were used according to the manufacturer's instructions. For the pure visualization of protein bands, silver nitrate staining was performed, as previously described by Shevchenko *et al.*[3] Gel images were digitized using a digital camera. The Western blots were prepared using the Trans-Blot Turbo Transfer System from BioRad. Proteins were transferred onto midi-size LF PVDF membranes for 10 min at 2.5 A and 25 V. The proper transfer of proteins to the PVDF membrane was verified

and documented using LICOR's Revert Total Protein Stain protocol (Doc # 988-19494). Control stains were scanned using the Odyssey® CLx Imaging System (LI-COR Biosciences) in the 700 nm channel at 84 µm resolution, medium intensity and auto adjust. All further steps were followed according to the Western blot protocol of LI-COR (Doc # 988-19647). The detection of the specific proteins was performed with primary and secondary antibodies indicated in Table 3 using the respective incubation conditions. Detection of the specific signals was performed using the Odyssey® CLx Imaging System in the 800 nm channel at 84 µm resolution, medium intensity and auto adjust.

Supplemental Table 3: Used antibodies

Target	Primary antibody	Dilution and incubation conditions	Secondary antibody	Dilution and incubation conditions
HSP90-alpha class A member 1 (Entrez Gene ID 3320)	HSP90 Rabbit Polyclonal antibody IgG (Proteintech No: 13171-1-AP	1:4000 / room temperature / overnight	Licor Goat anti-Rabbit IRDye 800CW No. 926-32211	1:10000 / room temperature / 1 h
HSP90AB1class B member 1 (Entrez Gene ID 3326)	HSP90AB1 Rabbit Polyclonal IgG (Proteintech No: 11405-1-AP)	1:4000 / room temperature / overnight	Licor Goat anti-Rabbit IRDye 800CW No. 926-32211	1:10000 / room temperature / 1 h
GRP94-beta (Entrez Gene ID7184)	GRP94 Rabbit Polyclonal IgG (Proteintech No: 14700-1-AP)	1:4000 / room temperature / overnight	Licor Goat anti-Rabbit IRDye 800CW No. 926-32211	1:10000 / room temperature / 1 h
14-3-3-Epsilon (Entrez Gene ID 7531)	14-3-3-Epsilon Rabbit Polyclonal IgG (Proteintech No: 11648-2-AP)	1:4000 / room temperature / overnight	Licor Goat anti-Rabbit IRDye 800CW No. 926-32211	1:10000 / room temperature / 1 h
Tubulin alpha-1B (Entrez Gene ID 10376)	Tubulin alpha-1B Rabbit Polyclonal IgG (Invitrogen No PA5-21979)	1:3000 / room temperature / overnight	Licor Goat anti-Rabbit IRDye 800CW No. 926-32211	1:10000 / room temperature / 1 h
Histone H4 (Entrez Gene ID 8367)	Histone H4 Rabbit Polyclonal IgGG (Proteintech No: 16047-1-AP)	1:500 / 4°C/ overnight	Licor Goat anti-Rabbit IRDye 800CW No. 926-32211	1:10000 / room temperature / 1 h
YWHAZ (Entrez Gene ID 7534)	YWHAZ Rabbit Polyclonal IgG (Proteintech No: 14881-1-AP)	1:4000 / room temperature / overnight	Licor Goat anti-Rabbit IRDye 800CW No. 926-32211	1:10000 / room temperature / 1 h
Vimentin (Entrez Gene ID 7431)	Vimentin Rabbit Polyclonal IgG	1:10000 / room temperature / overnight	Licor Goat anti-Rabbit IRDye 800CW	1:10000 / room

	(Invitrogen No: PA5-27231)		No. 926-32211	temperature / 1 h
PSMA4 (Entrez Gene ID 5685)	20S Proteasome alpha4 (H-4)_ Mouse Monoclonal IgG (Santa Cruz Biotech., INC. No: sc-271297)	1:1000 / room temperature / overnight	Licor Goat anti-Mouse IRDye 800CW No. 926-32210	1:10000 / room temperature / 1 h
PSMB5 (Entrez Gene ID 5693)	PSMB5 (D1H6B) Rabbit Monoclonal IgG (Cell Signaling Technology No:12919)	1:1000 / room temperature / overnight	Licor Goat anti-Rabbit IRDye 800CW No. 926-32211	1:10000 / room temperature / 1 h
PSMB6 (Entrez Gene ID 5694)	PSMB6 (E1K9O) Rabbit monoclonal IgG (Cell Signaling Technology No: 13267)	1:1000 / room temperature / overnight	Licor Goat anti-Rabbit IRDye 800CW No. 926-32211	1:10000 / room temperature / 1 h

LC-MS/MS and data analysis

LC-MS/MS experiments were performed on an Orbitrap Exploris™ 480 mass spectrometer (Thermo Scientific, Bremen, Germany) coupled to an Ultimate™ 3000 RSLCnano HPLC (Dionex/ Thermo Scientific, Waltham, MA, USA). Chromatographic separation of tryptic peptides was achieved by a 60 min linear gradient using a binary buffer system that consisted of: 0.1 % (v/v) acetic acid in HPLC-grade water; 100 % ACN in 0.1 % (v/v) acetic acid with increasing concentrations of acetonitrile (7-25 % (v/v) in 0.1 % (w/v) acetic acid) on a reverse phase column (Accucore 150-C18, 25 cm x 75 µm, 2.6 µm C18, 150 Å), at a flow rate of 300 nL/min at 40 °C. The MS scans were carried out in a m/z range of 350 to 1200 m/z.

For data acquisition in data independent mode (DIA) (ChAdOx1 nCoV-19 or Ad26.COV2.S vaccine lot analysis), precursor scans were acquired at a resolution of 120,000 and fragments at a resolution of 30.000 in 66 windows with 13 m/z and a window overlap of 2 m/z. For detailed information see Supplementary Table 4. The mass spectrometry proteomics data have been deposited to the ProteomeXchange Consortium via the PRIDE[4] partner repository with the dataset identifier PXD027344.

Supplemental Table 4: Parameters for LC-MS/MS analyses

reversed phase liquid chromatography (RPLC)

instrument	Ultimate 3000 RSLC (Thermo Scientific)
trap column	75 µm inner diameter, packed with 3 µm C18 particles (Acclaim PepMap100, Thermo Scientific)
analytical column	Accucore 150-C18, (Thermo Fisher Scientific) 25 cm x 75 µm, 2,6 µm C18 particles, 150 Å pore size
buffer system	binary buffer system consisting of 0.1 % acetic acid in HPLC-grade water (buffer A) and 100 % ACN in 0.1 % acetic acid (buffer B)
flow rate	300 nl/min
gradient	linear gradient of buffer B from 2 % up to 25 %
gradient duration	60 min
column oven temperature	40 °C
Mass spectrometry	
instrument	Orbitrap Exploris™ 480
electrospray	Nanospray FlexTM Ion Source
operation mode	data-independent
Full MS	
MS scan resolution	120000
AGC target	3e6
maximum ion injection time for the MS scan	60 ms
Scan range	350 to 1200 m/z
RF Lens	50 %
Spectra data type	profile
dd-MS2	
Resolution	30,000
MS/MS AGC target	3e6
maximum ion injection time for the MS/MS scans	auto
Spectra data type	profile

microscans	1
isolation window	66
Fixed first mass	200
dissociation mode	higher energy collisional dissociation (HCD)
Normalized collision energy	30 %

The data were analyzed with Spectronaut version 14.10.201222.47784 (Biognosis, Zurich, Switzerland) in directDIA mode using the human Uniprot database (version 01/2021) with added SARS-CoV-2 spike protein (YP_009724390.1) sequence and protein sequences of ChAdOx1 nCoV-19 vector consisting of chimpanzee adenovirus Y25 (NC_017825) with exchanged regions (E4ORF4, E4ORF6, E4ORF6/7) from human adenovirus 5 (AC_000008) for the ChAdOx1 nCoV-19 analysis. For the Ad26.COV2.S analysis we used a database comprised of human Uniprot database (version 01/2021) with added SARS-CoV-2 spike protein (YP_009724390. 1) sequence and protein sequences of hAd26 (Uniprot taxon identifier ID 46928) with exchanged regions (E4ORF6/7) from human adenovirus 5 (AC_000008).

Identifications were based on a precursor Q-value cut-off of 0.001 and a $FDR_{protein}$ of 0.01. The complete Spectronaut parameters are listed in Supplementary Table 3.

Supplementary Table 5: Spectronaut parameters.

Parameter level	Parameter	Setting
Peptides	Toggle N-terminal M	TRUE
Peptides	Min Peptide Length	7
Peptides	Max Peptide Length	52
Peptides	Missed Cleavages	2
Peptides	Digest Type	Specific
Peptides	Enzymes / Cleavage Rules	Trypsin/P
Data Extraction	MS1 Mass Tolerance Strategy	Dynamic
Data Extraction	MS1 Mass Tolerance Strategy - Correction Factor	1
Data Extraction	MS2 Mass Tolerance Strategy	Dynamic
Data Extraction	MS2 Mass Tolerance Strategy - Correction Factor	1
XIC Extraction	XIC IM Extraction Window	Dynamic
XIC Extraction	XIC IM Extraction Window - Correction Factor	1
XIC Extraction	RT IM Extraction Window	Dynamic
XIC Extraction	RT IM Extraction Window - Correction Factor	1

Modifications	Max Variable Modifications	5
Modifications	Select Modifications - fixed Modifications	Carbamidomethyl (C)
Modifications	Select Modifications - variable Modifications	Oxidation (M)
Calibration	MS1 Mass Tolerance Strategy	System Default
Calibration	MS2 Mass Tolerance Strategy	System Default
Identification	Machine Learning	Per Run
Identification	Precursor PEP Cutoff	1
Identification	Protein Qvalue Cutoff	0.01
Identification	Exclude Single Hit Proteins	FALSE
Identification	PTM Localization	TRUE
Identification	PTM Localization - Probability Cutoff	0.75
Identification	P-value Estimator	Kernel Density Estimator
Identification	Precursor Qvalue Cutoff	0.001
Identification	Single Hit Definition	By Stripped Sequence
Quantification	Interference Correction	TRUE
Quantification	Best N Fragments per Peptide	TRUE
Quantification	Best N Fragments per Peptide - Min	6
Quantification	Best N Fragments per Peptide - Max	10
Quantification	Quantity MS-Level	MS2
Quantification	Quantity Type	Area
Quantification	Data Filtering	Qvalue
Quantification	Data Filtering - Imputing Strategy	No Imputing
Quantification	Cross Run Normalization	FALSE
Workflow	MS2 DeMultiplexing	Automatic
Workflow	Run Limit for directDIA Library	-1
Workflow	Profiling Strategy	iRT Profiling
Workflow	Profiling Strategy - Profiling Row Selection	Minimum Qvalue Row Selection
Workflow	Profiling Strategy - Profiling Row Selection - Qvalue Threshold	0.001
Workflow	Profiling Strategy - Profiling Target Selection	Profile only non-identified Precursor
Workflow	Profiling Strategy - Profiling Target Selection - Identification Criterion	Qvalue
Workflow	Profiling Strategy - Profiling Target Selection - Threshold	0.001
Workflow	Profiling Strategy - Carry-over exact Peak Boundaries	FALSE
Workflow	Profiling Strategy - Unify Peptide Peaks Strategy	Select corresponding Peak

The Spectronaut unique protein iBAQ intensities (filtered for at least 3 peptides per protein with ion Qvalues < 0.001) were cleared for preparation contaminants (trypsin, keratin, dermicidin) used for a comparison of samples[19].

Data analysis and generation of plots was carried out using R[5] (version 4.0.2) depending on the tidyverse (version 1.3.0)[6] and scales (version 1.1.1).

Purification or fractionation of adenovirus particles from the vaccine

The first step was a sucrose cushion ultracentrifugation. 1 to 6 ml vaccine were diluted in buffer (phosphate buffer) to 15 ml and loaded slowly over 2 ml 15 % sucrose solution (phosphate buffered; 17 ml tube, opaque, Beckman Coulter) forming a layer and centrifuged at 20.000 rpm, 12 °C for 2 hours with SW32Ti rotor in a Beckman Coulter Optima L-100XP. The supernatant was discarded and the resulting pellet was layered with buffer (1/10 of the starting volume of the vaccine) and incubated overnight at 4 °C.

The second step was a sucrose gradient ultracentrifugation. The resuspended pellet was loaded on a 5 to 50 % sucrose gradient (phosphate buffered; 17 ml tube, ultra-clear, Beckman Coulter) that was prepared the day before for equilibration. For centrifugation, the same conditions were used as mentioned above. The resulting distinct and adenovirus-rich band was isolated.

The last step was ultracentrifugation for pelleting of adenovirus particles. The isolated band was diluted in buffer to 4 ml volume and centrifuged (4 ml tube, opaque, Beckman Coulter) at 12.000 rpm, 12 °C for 2 hours with SW60Ti rotor. The supernatant was discarded and the resulting pellet was layered with buffer (1/10 of the starting volume of the vaccine) and incubated overnight at 4 °C.

For the fractionation experiments, ultracentrifugation was performed at 20.000 rpm (=53750 x g, SW60 rotor), at 12 °C for 2 hours and the pellet was resuspended in 1/10 of the starting volume with PBS buffer. Phosphate buffer: 50 mM $Na_2HPO_4*2H_2O$ pH 7.4, 150 mM NaCl.

Finally, the quality of each batch was analyzed by transmission electron microscopy (TEM) as described below.

Proteasome activity assays

ChAdOx nCoV-19, Ad26.COV2.S and HEK293 cell lysates were tested for proteasomal activity. HEK293 cells were gently lysed by repeated freeze-thaw cycles in buffer containing 10 mM Tris (pH 7.0), 25 mM KCl, 10 mM NaCl, 1.1 mM $MgCl_2$, 1 mM DTT, 10 % glycerol, and protease inhibitor cocktail Complete (Sigma-Aldrich). Chymotrypsin-like activity was assessed in 50 µl vaccine or HEK293 cell lysate (0.25 µg) using 0.2 mM fluorescently tagged substrate Suc-LLVY-AMC (Bachem, Bubendorf, Switzerland). To confirm proteasomal activity 100 nM Bortezomib

(Selleckchem, Houston, Texas, United States), an inhibitor of chymotrypsin-like activity[7] or Carfilzomib[8] (Selleckchem, Houston, Texas, United States), was added. The free AMC fluorescence was quantified with a fluorometer using a 380/460 nm filter set (Fluorescence spectrometer Infinite M200 Pro, software i-control1.7; TECAN, Männerdorf, Switzerland). Increase of fluorescence was measured over 2 hours. Proteasome turnover was determined by calculating the rise of the linear slope at the beginning of the measurement (substrate turnover (Δ RFU/min)).

Dynamic Light Scattering and Zeta Potential Measurements

All dynamic light scattering (DLS) measurements were performed in a fixed scattering angle Zetasizer Nano-S system (Malvern Instruments Ltd., Malvern, UK). The hydrodynamic diameter (nm) was measured at 25 °C, and light scattering was detected at 173° and three repeating measurements consisting of 12 runs of 10 seconds each. Experimental data were collected from at least three independent experimental replicates. For all DLS measurements, non-purified ChAdOx1 nCoV-19, purified ChAdOx1 nCoV-19 and Ad26.COV2.S vaccine was diluted at a ratio of 1:10 in sterile-filtered 0.9 % NaCl supplemented with 4 mg/mL D(+) sucrose (RNase/DNase free; Cat. No. 9097.1, Carl Roth GmbH, Germany). Assessment of changes in the hydrodynamic diameter of ChAdOx1 nCoV-19 vector in the presence of PF4 was performed by incubating 10 and 50 µg/mL of human PF4 (Chromatec, Greifswald, Germany) with ChAdOx1 nCoV-19 vaccine at RT for five minutes before DLS measurements. For titration experiments, either 1:10 diluted ChAdOx1 nCoV-19 or Ad26.COV2.S vaccine was incubated with increasing concentrations of PF4 from 1, 5, 10,15, 20, 25, and 50 µg/mL. Similarly, PF4 at a fixed concentration of 10 µg/mL was incubated with ChAdOx1 nCoV-19 vaccine with decreasing dilutions of 1:1000, 1:750, 1:500, 1:250, 1:100, 1:50. 1:25 and 1:10. Dissociation of complexes formed between ChAdOx1 nCoV-19 vector and added components was achieved by 1 IU/ml unfractionated heparin (UFH, Ratiopharm GmbH, Ulm, Germany). In a subset of experiments, undiluted vaccine, their supernatant and dilution adjusted pellet fractions were used and dissociation of complexes was achieved by 10 IU/ml UFH. Surface zeta potential (ζ, mV) was performed in folded capillary zeta cells (DTS1070, Malvern Instruments Ltd., Malvern, UK). It consisted of three runs, each with 20 measurements at a voltage set to 10 V.

Data analysis was performed using Zetasizer software, Version 7.13 (Malvern Instruments Ltd., Malvern, UK). Statistical analysis and data plots were prepared with GraphPad Prism version 9.0.0 for Windows. Differences between groups were considered significant after assessment by ordinary one-way ANOVA with Sidak's multiple comparisons test, with Alpha set to 0.05.

Immunoelectron microscopy and transmission electron microscopy

For TEM, the vaccine or the purified adenovirus particles was incubated with biotinylated PF4 (10 ng/ml in phosphate buffer; PF4-biotin) for at least 1 hour at room temperature. After that, the sample was transferred to formvar coated TEM grids (400 mesh, Plano GmbH), washed with phosphate buffer and blocked with phosphate buffer containing 1 % BSA. On the one hand, samples were labeled with an anti-Adenovirus mAb (Abcam, ab7428, 1:500) for 1 hour at room temperature and an anti-mouse gold conjugate (BBI Solutions, GMHL10, 10 nm, 1:50) as secondary antibody. On the other hand, the same samples were labeled with a streptavidin-gold conjugate (Sigma, 10 nm, 1:10) for the staining of PF4-biotin for 45 min at room temperature.

All grids were stained with 1 % phosphotungstic acid at pH 7.4 and analyzed with a Tecnai-Spirit TEM (FEI, Eindhoven) at an accelerating voltage of 80 kV. The same procedure was used for preparing the controls, vaccine and PF4-Biotin.

For analysis of preparation quality after the purification of ChAdOx1 nCoV-19 the samples were transferred to formvar coated TEM grids (400 mesh, Plano GmbH), stained with 1 % phosphotungstic acid at pH 7.4 and analyzed with a Tecnai-Spirit TEM (FEI, Eindhoven) at an accelerating voltage of 80 kV.

Immunofluorescence staining

10 µg/ml human PF4 (Chromatek, Greifswald, Germany) was incubated with 1:10 diluted ChAdOx1 nCoV-19 (AstraZeneca, lots ABV5443, ABW0018, ABV5297) or Ad26.COV2.S (Johnson and Johnson, lots 21C11-01, 21C10-01, XD955) in 2 mg/ml sucrose in 0.9 % injection-grade NaCl. After 5 minutes incubation at room temperature, 10 µl were spread on beforehand washed (subsequent sonication in 99 % EtOH, 17 % HCl in 50 % MeOH, ultrapure water, 99 % EtOH) 22x22mm #1.5 high-precision coverslips (VWR, Germany). Slides were air-dried at room temperature and fixed with 2 % electron microscopy-grade paraformaldehyde

(Thermo Fisher Scientific) in 4 % sucrose-containing PEM-buffer (80 mM PIPES, 5 mM EGTA, 2 mM $MgCl_2$) for 5 min at room temperature. Slides were blocked with 2 % fetal bovine serum, 2 % bovine serum albumin, 0.1 % cold fish gelatin and 2 % normal goat serum in 1x PBS pH 7.4 for 45 min at room temperature. For detection of PF4, a mouse monoclonal IgG2b (RTO clone, Thermo Fisher, MA5-17639) diluted to 2 µg/ml in 2 % bovine serum albumin in 1x PBS pH 7.4, was incubated for 30 min at room temperature under gentle agitation. Bound primary antibodies were detected after several washes in 1x PBS using AlexaFluor 488-conjugated secondary antibodies (A11001, Thermo Fisher Scientific) at 1:500 dilution for 30 min at room temperature. For detection of the hexon polypeptide, a custom Cy5-conjugated (Lightning-Link Cy5 conjugation kit according to manufacturer's description (Novus Biologicals, 781-0010)) IgG2a antibody (abcam, ab7428) was incubated at 1 µg/ml in 2 % bovine serum albumin for 1 hour at room temperature. Slides were collected in 1x PBS and stored at 4 °C in the dark upon mounting and imaging. Antibody specificity was checked beforehand using secondary immunofluorescence with minus primary antibody control.

Single-molecule light microscopy (SMLM): Direct stochastical optical reconstruction microscopy (dSTORM)

Before imaging, coverslips were washed in ultrapure water and 100 nm multi-fluorescent Tetraspek Beads (Thermo Fisher) were added in a 1:800 dilution in ultrapure water for 5 min at room temperature. After one wash in electron microscopy-grade water, coverslips were inversely mounted on depression microscopy glass slides (VWR, Germany) in Everspark dSTORM buffer (Idylle Labs, Paris, France) containing deoxygenized 100 mM mercaptoethanolamin hydrochloride (MEA) in TRIS buffer pH 8[23]. Coverslips were sealed airtight with TwinSil two-component dental silicone. Care was taken that mounting time did not exceed 30 seconds to minimize oxygenation of the buffer. Slides were imaged after between 1 hour and 1 week of incubation with the imaging buffer and were stored at 4°C in the dark.

For dSTORM imaging, a Zeiss Elyra PS.1 super-resolution system was used with a temperature-controlled chamber set to 30 °C. To equilibrate instruments and reduce drift, the system was switched on at least two hours before imaging. Samples were

equilibrated for at least 20 minutes in the imaging chamber. The objective used was a Zeiss, Apochromat, 63x, 1.4 NA TIRF objective, and emitted fluorescence was projected on an Andor iXon 897 EMCCD camera with a 512x512 pixel chip, resulting in an effective pixel size of 160 nm. Areas of interest with at least two fiducial markers per field of view were selected using the epifluorescence mode. Z-drift compensation was performed with the Definite Focus system set on continuous compensation. During continuous TIRF-HP-illumination, the laser power was gradually increased to bleach fluorophores until steady-state single-molecule photoswitching was observed. 256x256 pixels frames were acquired at a framerate of 55 Hz with a manual gain set to between 20 and 40. Subsequently, 14,000 frames image sequences of the same field of views of the Cy5 and AF488 fluorophores were recorded, saved as .czi files and imported to FIJI[9] using the BioFormats importer. After import, raw data was saved as .nji files using the NanoJ core toolbox[10]. Raw single-channel dSTORM data was initially drift-corrected with the built-in function of the NanoJ core plugin. Chromatic aberration between both channels was estimated on intensity-averaged frames of the drift-corrected data (to clearly visualize fiducial markers) and corrected on drift-corrected source data using the Channel Registration function of NanoJ core. After drift correction and sub-pixel channel registration, image sequences were cropped to 10,000 frames of 200x200 pixels before performing emitter-localization analysis. Cropped, drift-corrected and channel-registered data was exported with NanoJ core as .nji files.

For both channels, blinking events were detected, and x-y localized with the Thunderstorm algorithm[11] using normalized Gaussian fitting with a 3 px fitting radius, weighted least-squares fitting method, an initial Sigma of 1.6 px, and multi-emitter fitting analysis disabled. The resulting localization table was exported as .csv files and uncertainty- as well as sigma-filtered. Data was then density-filtered with a minimum distance radius of 50 nm with a minimum of 5 neighbors in the radius. The resulting localization data was visualized either using the built-in averaged shifted histograms function with 10x magnification or as well as the scatter plot function with 50x magnification (with herein hexon-localizations density-filtered with a minimum of 50 neighbors in a distance radius of 50 nm). Single-channel data was visualized using the inverted NanoJ-orange LUT or merged and exported using basic FIJI functions.

Image analysis

To analyze PF4-molecule aggregation on adenoviral capsid clusters, PF4 particle density in- and outside boundaries of adenoviral complexes were quantified. To automate this, an ImageJ1-macro script was developed.[9] In brief, dual-channel 50x magnified single-molecule scatterplots were imported to FIJI, adenoviral clusters gaussian-blurred and thresholding-based binarized. A ring-like reference region outside (500 nm outside the adenoviral particles, width of 500 nm) of each complex was defined which did not contain adenoviral localizations. Then, PF4 localizations in each region of interest (ROI, inside adenoviral particles, and outside on glass as internal reference) were counted and normalized to the ROI area as particle density. To account for preparation-based differences in local molecule density, PF4 density ratios of the matching ROIs (inside/outside AV) were calculated and normalized to the median of every group outside ROI density ratio. ImageJ macro scripts are available on http://www.github.com/siegerist.

Statistical analysis and data visualization were performed with Prism 9.1.2 (GraphPad Software, San Diego, California USA): Normality was checked using Kolmogorov-Smirnov testing. For >2 groups and non-parametric data, differences between groups were checked using Kruskal-Wallis-test with Dunn's multiple comparison test. P-values are indicated in the respective plots, where not indicated, p-values were >0.05.

Zebrafish vascular permeability assay

Zebrafish maintenance was performed as described previously.[12] All experiments were performed in accordance with German animal protection law overseen by the "Landesamt für Landwirtschaft, Lebensmittelsicherheit und Fischerei, Rostock" of the federal state of Mecklenburg - Western Pomerania. In order to track vascular leakage, Tg(-3.5fabp10a:gc-eGFP)[13] (ZFIN-ID: ZDB-FISH-150901-8595) and Tg(-3.5fabp10a:gc-eGFP); mitfa$^{w2/w2}$ were used.[14] Larvae at 5 days post fertilization were anesthetized with 0.02 % tricaine (MS-222, Sigma-Aldrich) and placed laterally on a custom-made agarose dish. As demonstrated in Supplementary Video 1, approximately 1 nl intramuscular injections of 0.9 % NaCl, 100 µM EDTA, ChAdOx1 nCoV-19 (lot: ABV5297) and Ad26.COV2.S (lot: XD955 and 21C10-01) were performed with glass capillaries (Femtotips I, Eppendorf AG, Hamburg, Germany)

attached to a Transjector 5246 (Eppendorf AG) into four adjacent myotomes caudal of the cloaca in each larva. Afterward, larvae were embedded laterally in 0.6 % agarose (LE agarose, Biozym, Hessisch Oldendorf, Germany) with the injection side facing up and covered with E3 medium containing 0.02 % tricaine. Imaging was performed with a P2-SHR Plan Apo 1x objective attached to an SMZ18 fluorescence stereomicroscope equipped with a motorized Z-drive (Nikon GMBH, Düsseldorf, Germany) and an X-Cite Xylis LED (Excelitas, Göttingen, Germany). Z-Stacks with 10 frames for each larva were acquired with 470 nm slice-to-slice distance with a 135x magnification in the caudal region at 0 and 10 min post-injection (p.i.). Z-Stacks were converted to maximum intensity projections (MIPs) and stacks of two MIPs for both timepoints were created. Fluorescence intensity measurements were performed with 4 custom ROIs for each injected myotome. The same ROIs were used to obtain the fluorescence intensity of the adjacent caudal vein in order to calculate a muscle to vessel ratio. The t=0 of each larva served as normalizer for the 10 min p.i. ratio and displays the leakage of eGFP into the musculature. Creation of MIPs, Stacks and measurements were performed with ImageJ (National Institutes of Health, Bethesda, MD, USA)). Statistical analysis was performed in Prism 9.1.2 (GraphPad Software, San Diego, California USA). After checking gaussian distribution with a Kolmogorov-Smirnov test, differences between groups were checked using Kruskal-Wallis-test with Dunn’s multiple comparisons.

References

1. Nickerson JL, Doucette AA. Rapid and Quantitative Protein Precipitation for Proteome Analysis by Mass Spectrometry [eng]. Journal of proteome research. 2020;19(5):2035–42.
2. Blankenburg S, Hentschker C, Nagel A, Hildebrandt P, Michalik S, Dittmar D, et al. Improving Proteome Coverage for Small Sample Amounts: An Advanced Method for Proteomics Approaches with Low Bacterial Cell Numbers. Proteomics. 2019;19(23):e1900192.
3. Shevchenko A, Wilm M, Vorm O, Mann M. Mass spectrometric sequencing of proteins silver-stained polyacrylamide gels. Analytical chemistry. 1996;68(5):850–8.
4. Perez-Riverol Y, Csordas A, Bai J, Bernal-Llinares M, Hewapathirana S, Kundu DJ, et al. The PRIDE database and related tools and resources in 2019: improving support for quantification data [eng]. Nucleic acids research. 2019;47(D1):D442-D450.
5. R Core Team. R: A language and environment for statistical computing. R Foundation for Statistical Computing, Vienna, Austria.: Available online at https://www.R-project.org/; 2018.
6. Wickham H, Averick M, Bryan J, Chang W, McGowan L, François R, et al. Welcome to the Tidyverse. JOSS. 2019;4(43):1686.
7. Berkers CR, Verdoes M, Lichtman E, Fiebiger E, Kessler BM, Anderson KC, et al. Activity probe for in vivo profiling of the specificity of proteasome inhibitor bortezomib. Nature methods. 2005;2(5):357–62.
8. Arastu-Kapur S, Anderl JL, Kraus M, Parlati F, Shenk KD, Lee SJ, et al. Nonproteasomal targets of the proteasome inhibitors bortezomib and carfilzomib: a link to clinical adverse events [eng]. Clinical cancer research : an official journal of the American Association for Cancer Research. 2011;17(9):2734–43.
9. Schindelin J, Arganda-Carreras I, Frise E, Kaynig V, Longair M, Pietzsch T, et al. Fiji: an open-source platform for biological-image analysis. Nature methods. 2012;9(7):676–82.

10. Laine RF, Tosheva KL, Gustafsson N, Gray RDM, Almada P, Albrecht D, et al. NanoJ: a high-performance open-source super-resolution microscopy toolbox [eng]. Journal of physics D: Applied physics. 2019;52(16):163001.
11. Hoboth P, Šebesta O, Sztacho M, Castano E, Hozák P. Dual-color dSTORM imaging and ThunderSTORM image reconstruction and analysis to study the spatial organization of the nuclear phosphatidylinositol phosphates. MethodsX. 2021;8:101372.
12. Müller T, Rumpel E, Hradetzky S, Bollig F, Wegner H, Blumenthal A, et al. Non-muscle myosin IIA is required for the development of the zebrafish glomerulus [eng]. Kidney international. 2011;80(10):1055–63.
13. Xie J, Farage E, Sugimoto M, Anand-Apte B. A novel transgenic zebrafish model for blood-brain and blood-retinal barrier development. BMC developmental biology. 2010;10:76.
14. Siegerist F, Zhou W, Endlich K, Endlich N. 4D in vivo imaging of glomerular barrier function in a zebrafish podocyte injury model. Acta physiologica (Oxford, England). 2017;220(1):167–73.